Tourmaline Reference Materials for the In Situ Analysis of Oxygen and Lithium Isotope Ratio Compositions

PROF. HORST R. MARSCHALL (Orcid ID : 0000-0002-0609-682X)

Article type : Original Article

Tourmaline Reference Materials for the *In Situ* Analysis of Oxygen and Lithium Isotope Ratio Compositions

Michael **Wiedenbeck** (1)*, Robert B. **Trumbull** (1), Martin **Rosner** (2, 12), Adrian **Boyce** (3), John H. **Fournelle** (4), Ian A. **Franchi** (5), Ralf **Halama** (6, 13), Chris **Harris** (7), Jack H. **Lacey** (8), Horst **Marschall** (9, 14), Anette **Meixner** (10), Andreas **Pack** (11), Philip A.E. **Pogge von Strandmann** (9, 15), Michael J. **Spicuzza** (4), John W. **Valley** (4) and Franziska D.H. **Wilke** (1)

(1) GFZ German Research Centre for Geosciences, 14473 Potsdam, Germany

(2) Department of Marine Chemistry and Geochemistry, Woods Hole Oceanographic Institution, Woods Hole, MA 02543, USA

(3) Scottish Universities Environmental Research Centre, East Kilbride G75 0QF, UK

(4) Department of Geoscience, University of Wisconsin, Madison, WI 53706, USA

(5) School of Physical Sciences, Open University, Milton Keynes MK7 6AA, UK

(6) Department of Geology, University of Maryland, College Park, MD 20742, USA

(7) Department of Geological Sciences, University of Cape Town, Rondebosch 7701, South Africa

(8) National Environmental Isotope Facility, British Geological Survey, Keyworth NG12 5GG, UK

(9) Bristol Isotope Group, School of Earth Sciences, University of Bristol, Bristol BS8 1RJ, UK

(10) Faculty of Geosciences & MARUM - Center for Marine Environmental Sciences, University of Bremen, 28359 Bremen, Germany

(11) Geowissenschaftliches Zentrum, Universität Göttingen, 37077 Göttingen, Germany

(12) Current address: IsoAnalysis UG, 12489 Berlin, Germany

(13) Current address: School of Geography, Geology and Environment, Keele University, Keele ST5 5BG, UK

(14) Current address: Institut für Geowissenschaften, Goethe-Universität, 60438 Frankfurt am Main, Germany

(15) Current address: Institute of Earth and Planetary Sciences, University College London and Birkbeck, University of London, London WC1E 6BS, UK

This article has been accepted for publication and undergone full peer review but has not been through the copyediting, typesetting, pagination and proofreading process, which may lead to differences between this version and the Version of Record. Please cite this article as doi: 10.1111/GGR.12362

* Corresponding author. e-mail: michael.wiedenbeck@gfz-potsdam.de

Three tourmaline reference materials sourced from the Harvard Mineralogical and Geological Museum (schorl 112566, dravite 108796 and elbaite 98144), which are already widely used for the calibration of *in situ* boron isotope measurements, are characterised here for their oxygen and lithium isotope compositions. Homogeneity tests by secondary ion mass spectrometry (SIMS) showed that at sub-nanogram test portion masses their $^{18}O/^{16}O$ and $^{7}Li/^{6}Li$ isotope ratios are constant within ± 0.27‰ and ± 2.2‰ (1*s*), respectively. The lithium mass fractions of the three materials vary over three orders of magnitude. SIMS homogeneity tests showed variations in $^{7}Li/^{28}Si$ between 8% and 14% (1*s*), which provides a measure of the heterogeneity of the Li contents in these three materials. Here we provide recommended values for $\delta^{18}O$, $\Delta'^{17}O$ and $\delta^{7}Li$ for the three Harvard tourmaline reference materials based on results from bulk mineral analyses from multiple, independent laboratories using laser- and stepwise fluorination gas mass spectrometry (for O), and solution multi-collector inductively coupled plasma-mass spectroscopy (for Li). These bulk data also allow us to assess the degree of inter-laboratory data that might be present in such datasets. This work also re-evaluates the major element chemical composition of the materials by electron probe microanalysis and investigates the presence of a chemical matrix effect on SIMS instrumental mass fractionation with regards to $\delta^{18}O$ determinations, which was found to be < 1.6‰ between these three materials. The final table presented here provides a summary of the isotope ratio values that we have determined for these three materials. Depending on their starting mass either 128 or 256 splits have been produced of each material, assuring their availability for many years into the future.

Keywords: tourmaline, lithium isotopes, oxygen isotopes, reference materials, SIMS, matrix effect.

Received 15 May 20 – Accepted 08 Sep 20

In situ measurement of boron isotope ratios in tourmaline by SIMS and LA-ICP-MS has become a widely used method for investigating fluid-rock interaction in igneous, metamorphic and hydrothermal systems, with important applications to ore genesis studies. Some of this work has been summarised in reviews by Slack and Trumbull (2011), Marschall and Jiang (2011) and in various chapters of the monograph by Marschall and Foster (2018). The rapid growth of B isotope studies on tourmaline is partly due to the availability of well-characterised and demonstrably homogeneous tourmaline reference materials (RMs). Other stable-isotope systems that can be applied to tourmaline include H, Li and O, and these have shown their utility in several studies that employed bulk analysis of mineral separates (e.g., Taylor *et al.* 1999, Matthews *et al.* 2003, Siegel *et al.* 2016). However, the lack of characterised RMs that are known to be homogeneous at the nanogram to picogram sampling scale has prevented the application of *in situ* methods to these isotope systems. This is unfortunate, as the combination of two or more isotope systems can reduce ambiguities in models built on laboratory data. In this study we provide O- and Li-isotope ratio data for three tourmaline RMs so as to partially meet this need.

Oxygen has three stable isotopes: ^{16}O, ^{17}O and ^{18}O, which have natural abundances of *ca.* 99.76%, 0.04% and 0.2%, respectively. By convention, the two isotope ratios of oxygen are expressed in delta-notation relative to Standard Mean Ocean Water (SMOW) as follows:

$$\delta^{18}O = (^{18}O/^{16}O_{sample}/\ ^{18}O/^{16}O_{SMOW}) - 1 \qquad (1)$$

$$\delta^{17}O = (^{17}O/^{16}O_{sample}/\ ^{17}O/^{16}O_{SMOW}) - 1 \qquad (2)$$

where the absolute isotope abundance ratio for SMOW is set at $^{18}O/^{16}O = 0.00200520 \pm 0.00000045$ (Baertschi 1976) and $^{17}O/^{16}O = 0.0003799 \pm 0.0000008$ (Li *et al.* 1988). There is abundant literature documenting the utility of oxygen isotopes in identifying fluid provenance, constraining fluid/rock interaction and for isotope exchange geothermometry (e.g., Valley and Cole 2001, Valley 2003, Sharp *et al.* 2016). For most fractionation processes, $\delta^{17}O$ shows a close correlation with $\delta^{18}O$. However, small, mass-dependent deviations from such a correlation can now be resolved in terrestrial samples (Barkan and Luz 2005, Pack and Herwartz 2014). Such mass-dependent variations in $\delta^{17}O$ are a new tool in understanding oxygen isotope fractionation and/or reservoir-exchange processes (e.g., Herwartz *et al*. 2015, Sharp *et al*. 2016). Until now no

certified values are available for any silicate or oxide calibration material for $\delta^{17}O_{VSMOW}$, although recent efforts have been made to characterise San Carlos olivine and there are on-going efforts to standardise the treatment of such data (e.g., Pack *et al*. 2016, Sharp *et al*. 2016, Miller *et al*. 2020, Wostbrock *et al*. 2020). Although the efforts presented here do not represent an attempt at an ISO-compliant certification, we nonetheless believe they are a valuable contribution towards addressing this shortage.

Lithium has two stable isotopes, ^{6}Li and ^{7}Li, with natural abundances of *ca.* 7.6% and 92.4%, respectively, though their abundance ratio varies considerably in nature. For example, a difference of some 30‰ exists between unaltered MORB and seawater (e.g., Tomascak 2004). The Li isotope system can undergo large fractionation between geological materials (fluids, minerals, melts) during processes including fluid-rock interaction, fluid or melt unmixing, (re)crystallisation and diffusion, making it valuable for many geologic applications (e.g., Teng *et al.* 2004, Tomascak *et al.* 2016). Lithium isotope ratios are typically reported in δ-units (in ‰) with reference to lithium carbonate, L-SVEC (now NIST SRM-8545; Flesch *et al*. 1973, Brand *et al.* 2014) as follows:

$$\delta^{7}Li = (^{7}Li/^{6}Li_{sample}/ {}^{7}Li/^{6}Li_{L\text{-}SVEC}) - 1 \quad (3)$$

where the absolute isotopic abundance ratio for L-SVEC is set at $^{6}Li/^{7}Li = 0.08215 \pm 0.00023$ (combined uncertainty at coverage factor $k = 2$; Coplen 2011, Harms and Assonov 2018), equivalent to $^{7}Li/^{6}Li \approx 12.173$.

Both oxygen and lithium isotope ratios in tourmaline can readily be determined by SIMS on polished sample surfaces with a spatial resolution of < 20 µm and analytical repeatabilities at or below ± 1‰ (1*s*) in the case of $\delta^{7}Li$ and better than ± 0.2‰ (1*s*) in the case of $\delta^{18}O$. However, in practice such measurements are rarely made due to a lack of suitable tourmaline RMs. For this study we turned to the widely used Harvard tourmaline suite. Dyar *et al.* (2001) reported values of $\delta^{18}O$ for the tourmaline RMs elbaite, schorl and dravite studied here, albeit prior to the sample splitting done as part of the current investigation. Those analyses were done in one laboratory (Southern Methodist University) only and no isotope homogeneity tests for O isotopes were carried out at test portion masses relevant for microanalytical applications. Lin *et al*. (2019)

reported values of the Li isotope composition of the Harvard schorl and elbaite materials based on solution-nebulisation ICP-MS. Likewise, no isotope homogeneity tests were reported in that study. Finally, Dyar *et al*. (2001) also reported a single set of δD values for all three of the materials that are the focus of this current study (see below).

A particular concern in the determination of isotope amount ratios of light elements in tourmaline and other minerals where a wide major element compositional range exists is the possible presence of a chemical matrix effect. Bell (2009) discussed the chemical matrix effect in the context of SIMS Li isotope measurements in olivine. Because multiple and chemically diverse tourmaline RMs exist for B isotope analysis, workers have been able to demonstrate a small but significant chemical matrix effect in both SIMS (e.g., Kutzschbach *et al.* 2017, Marger *et al*. 2020) and ICP-MS applications (Míková *et al.* 2014). The issue of a matrix effect for the lithium and oxygen isotope SIMS analyses is discussed below.

Materials

Dyar *et al.* (2001) and Leeman and Tonarini (2001) reported on the major element compositions and chemical homogeneity of three megacrystic tourmaline samples from the Harvard Mineralogical and Geological Museum, designated elbaite, schorl and dravite (note: "dravite" is a misnomer, see below). Tonarini *et al.* (2003) and Gonfiantini *et al.* (2003) suggested a fourth natural tourmaline (IAEA-B4), which has a major element composition similar to that of the Harvard schorl, as a further RM for *in situ* chemical and B isotope analyses. We did not have access to large amounts of the B4 material with which to generate metrological splits, so we have not included this material in the current characterisation project. Hence, this study focussed exclusively on the three materials described below:

Elbaite (Harvard Mineralogical and Geological Museum #98144): This sample is from a 17.5 g single crystal collected from a granitic pegmatite in Minas Gerais, Brazil.

Schorl (HMGM #112566): This sample is from a 48.4 g single crystal collected from a granitic pegmatite in Zambezia Province, Mozambique (Hutchinson and Claus 1956).

Dravite (HMGM #108796): This sample has been previously described as a 16.6 g single crystal collected from alluvium in Madagascar (Dyar *et al*. 2001), but this mass seems to be erroneous. Based on its size (Frondel *et al.* 1966, gives 560 g as the mass) and locality, the sample was possibly derived from a granitic pegmatite. Of the amount of material provided to the first author by the Harvard Museum, two large, euhedral crystals with masses of 134 g and 194 g remain after producing our metrological splits (see below).

Based on the chemical analyses reported in Dyar *et al.* (2001) and in this study the schorl and elbaite samples are appropriately named, whereas the "dravite" term is misleading since this tourmaline has low Al contents, high Ca and an Fe/(Fe+Mg) ratio of ~ 0.5, whereby Fe^{3+} dominates and substitutes for Al (Frondel *et al.* 1966). Using the current nomenclature of Henry *et al*. (2011) this composition is an intermediate schorl-dravite-feruvite, but in the interests of historical consistency we will continue to refer to the HMGM #108796 material as "dravite". The chemical classifications of the three materials are shown in Figure 1. We note that the δD (Dyar *et al*. 2001) and $\delta^{11}B$ (Leeman and Tonarini 2001) have already been reported for these materials (see Table 7). More recently, Marger *et al*. (2020) have reported revised $\delta^{11}B$ bulk values for the three tourmaline materials (also shown on Table 7) that are as much as 1.6‰ lower than the values published previously.

We used a riffle splitter in order to generate ~ 100 mg units of < 2 mm fragments from single crystals from each of the three tourmaline specimens; these were placed in 0.5 ml screw-top plastic vials. In total we generated 256 vials of the elbaite, 128 vials of the schorl, and 512 vials of the dravite. In order to give these unique metrological identifiers, each set of splits has been given a Harvard catalogue number that is appended with an additional decimal place (i.e., 98144.1 Elbaite, 112566.1 Schorl and 108796.1 Dravite). With the exception of the wet chemical $\delta^{7}Li$ data, which were performed on fragments removed from the parent samples prior to splitting, all data reported here were made on tourmaline fragments taken from such vials of the split material.

Homogeneity assessments

Electron probe microanalysis (EPMA) for major elements

The characterisation study by Dyar *et al.* (2001) reported homogeneity testing in the form of EPMA traverses across single sections of the original crystals as well as mean values from four independent EPMA laboratories. Most of those reported EPMA analyses, however, showed very low analytical totals, which can be improved upon by utilising up-to-date EPMA procedures for optimal matrix correction accuracy. Also, there have been no data previously reported describing the chemical heterogeneity between random fragments that are more representative of each of the three materials. For this reason we conducted new EPMA analyses using a JEOL JXA8500F instrument at the GFZ Potsdam and a CAMECA SXFive FE instrument at the University of Wisconsin-Madison, both of which used a single vial of each tourmaline material prepared by riffle splitting during the current investigation. Both laboratories analysed six randomly selected fragments from a single split of each of the three tourmaline materials, whereby each fragment was analysed four times at broadly dispersed locations. In Madison, optically distinct (green vs. non-green) elbaite fragments were recognised and these were analysed separately (Table 1). Additional analyses at GFZ Potsdam were made of the silicate glass NIST SRM 610 for an "internal precision" and repeatability check.

The EPMA measurement results and method descriptions are reported in Table 1 and the full data set is available in online supporting information Table S1. Variations were found in the degree of homogeneity in these sets of fragments, making it difficult to define unique recommended values for the schorl and the dravite RMs. This is especially problematic for the elbaite RM, where the Madison EPMA results show distinct populations based on MgO, Al_2O_3 and FeO mass fractions for grains separated by colour (a distinction not made in the Potsdam contribution). Notwithstanding the variable homogeneity of the tourmaline RMs, the EPMA results of the two laboratories are in good agreement with each other and, with the exception of B_2O_3, with the previously reported mass fraction values in Dyar *et al*. (2001). The new EPMA results for B_2O_3 agree well with the values reported for non-EPMA techniques by Dyar *et al*. (2001). Thus, for schorl, the EPMA B_2O_3 "grand mean" values from Potsdam (10.1% *m/m* ± 0.4, 1*s*) and Madison (9.6% *m/m* ± 0.7, 1*s*) are consistent with the non-EPMA range of 9.7 to 10.3% *m/m*; for dravite the EPMA results are 10.1% *m/m* ± 0.5 (1*s*) for Potsdam and 9.9% *m/m* ± 0.5 (1*s*) for Madison, compared with the non-EPMA range of 10.0 to 10.3% *m/m* reported by Dyar *et al*. (2001). The inter-grain variability of the elbaite RM is relatively high for Fe, Mg and Al, but the variations for boron are no larger in elbaite than in the other two tourmaline RMs (Table 1).

Furthermore, the elbaite EPMA values from both laboratories are in good agreement with those of non-EPMA techniques from Dyar *et al*. (2001). The elbaite B_2O_3 "grand mean" value for Potsdam is 10.6 ± 0.5% *m/m* (1*s*), for Madison "non-green" and "green" populations the values are 10.1 ± 0.8% *m/m* and 10.0 ± 0.5% *m/m*, respectively; the range from non-EPMA techniques (Dyar *et al*. 2001 Table 4) is 10.1 to 10.2% *m/m*.

We conclude that schorl 112566.1, dravite 108796.1 and to a certain extent elbaite 98144.1 are suitable for use as EPMA calibration and quality control materials. Any particular fragment composition should fall within the bounds of the reported compositions in Table 1, provided at least 98% *m/m* of the composition (including Li, OH etc.) is accounted for in the EPMA matrix correction.

SIMS lithium testing

We used the Potsdam Cameca 1280-HR instrument to assess both the Li mass fraction and δ^7Li heterogeneities in the three tourmaline materials. For this purpose a mount was made that contained multiple fragments from each of the three tourmaline splits as well as a mm-sized piece of the NIST SRM 610 silicate glass. An additional benefit of this test is that these data contribute towards refining the absolute Li mass fractions reported by Dyar *et al*. (2001), which showed large discrepancies between analytical methods. However, we specifically note that we do not contribute any further absolute mass fraction data to this discussion.

Lithium mass fraction evaluation: Our SIMS analyses used a ~ 25 pA $^{16}O^-$ primary beam focussed to a ~ 2 µm diameter spot with a total impact energy of 23 keV. Data were collected using a 10 µm raster, thereby assuring a flat-bottom crater geometry. Each analysis was preceded by a 170 s pre-sputtering using a 2 nA primary beam and a 20 µm raster in order to locally remove the conductive gold coat and to suppress any surface contamination; actual data collection used a 10 µm raster, which was compensated with the instrument's dynamic transfer option. Prior to data collection we completed automatic centring routines on the field aperture in X and Y. The mass spectrometer was operated at a mass resolution of M/ΔM ≈ 3700, which is more than adequate to resolve both the $^6Li^1H^+$ ion from $^7Li^+$ and the $^{27}Al^1H^+$ ion from the $^{28}Si^+$ mass station. A 2000 × 2000 µm square field aperture, equivalent to a 20 × 20 µm field-of-view, and a 150 µm contrast aperture were used. The energy window was set to a 40 eV width and no offset voltage was

applied. Data were collected using a 40 μm wide entrance slit and a 280 μm wide exit slit running in mono-collection mode using the ETP pulse counting system, to which a synthetic 46.2 ns deadtime was applied using a delay circuit in our preamplifier. A single analysis consisted of twenty cycles of the peak stepping sequence $^{7}Li^{+}$ (2*s*), $^{28}Si^{+}$ (2*s*). A single analysis, including pre-sputtering, auto-centring and data acquisition, required 7 min. We conducted 116 such analyses over the course of one automated analysis sequence. Using these analytical conditions we had a typical $^{28}Si^{+}$ count rate of around 50,000 ions per second. The total amount of material removed during data acquisition was very small; our best estimate of the volume of the sputter crater, based on white light profilometry, is ~ 3.2 μm^3, equivalent to a test portion mass of ~ 10 pg. The dataset from this experiment, along with the Li mass fractions based on the calibration using the NIST SRM 610 glass, are shown in online supporting information Table S2. The equivalent Li_2O mass fractions in % *m/m*, along with other determinations from Dyar *et al.* (2001), are also given in Table 2. We explicitly note that the Li mass fractions reported here are not robust as the NIST SRM 610 silicate glass is, at best, a poor matrix match for the tourmalines we investigated.

Lithium isotope evaluation: Because Li mass fraction varied by a factor of 1000 between the elbaite and dravite materials (Table 2) it was not possible to run all three SIMS $\delta^{7}Li$ homogeneity experiments under identical conditions. To accommodate such large differences in mass fractions we modified the $^{16}O^{-}$ primary current, the ion detection system and the total count times, with the goal of achieving better than ± 0.2‰ (1*s*) measurement repeatability precision ("internal precision") on the individual analyses. Hence, the test portion masses, as determined by white light profilometry, also varied between materials. A summary of the specific analytical conditions is included in Table 3.

A common feature of all three sets of $^{7}Li^{+}/^{6}Li^{+}$ SIMS data is that the primary beam was operated in Gaussian mode with a total impact energy of 23 keV. Tests using a Köhler mode primary beam showed poor repeatability, and we therefore abandoned this approach. Pre-sputtering employed either a 20 or 30-μm raster, which was reduced to a 15 × 15 μm raster during data collection. The dynamic transfer option of the instrument was used to actively compensate for this rastering. Automatic beam centring on the field aperture in both X and Y was conducted before each analysis. The mass spectrometer was operated with a 40 eV energy window, using no energy offset, in conjunction with a mass resolving power $M/\Delta M > 1900$. Data were recorded in

multi-collection mode employing an NMR field control system. Ions were collected using the L2 and H2 trollies for $^{6}Li^{+}$ and $^{7}Li^{+}$, respectively; the actual detectors used varied between the experiments depending on Li mass fraction in the tourmaline RMs (see Table 3); for those experiments using electron multipliers we did an automatic voltage scan prior to each analysis so as to minimise drift due to aging of the first dynode. Analytical points were dispersed over multiple fragments in the epoxy mount and additionally, several points were placed closely together on a single fragment of the same tourmaline material as a "drift monitor" (DM) in order to test for a time dependent drift in the ion detection system. After setting all points, the analysis sequence of all non-DM points was randomised. Making the reasonable assumption that the RMs are homogeneous in isotopic composition within a confined area of a few hundred micrometres, the results of "drift monitor" determinations can also be used to quantify the repeatability of the given analytical design. The results from the lithium isotope ratio homogeneity tests of the three tourmaline materials are shown in Table 3, and the full set of results are available in Table S3.

The Li homogeneity assessment on the schorl material presented a special case in two respects. Firstly, the Li mass fraction in schorl is similar to that of the NIST SRM 610 silicate glass (Table 2). We therefore conducted interspersed $^{7}Li^{+}/^{6}Li^{+}$ determinations on this glass as a comparison test for the repeatability, whereby we assume that the NIST SRM 610 synthetic glass is homogeneous over the few hundred micrometres used for this assessment. Secondly, the schorl material was particularly challenging from the perspective of the ion count rates that it provided. Under the requirement that the $^{16}O^{-}$ primary beam current was in the range between 20 nA and 0.5 nA, it was found that one of the Li isotopes inevitably provided a count rate in the gap between optimum performance of our FC using a 10^{11} Ω resistor and the Hamamatsu pulse counting system (this "gap" is roughly between 2×10^{6} and 2×10^{5} counts per second). Ultimately, we elected to use a compromise where the $^{7}Li^{+}$ signal was towards the low end of the optimal range for our FC amplifier (3.9×10^{6} cps) and the $^{6}Li^{+}$ signal was slightly above the optimal range for our pulse counting system (3×10^{5} cps). An automatic voltage scan conducted on the Hamamatsu electron multiplier prior to each analysis was able to compensate the drift in the detector at the 0.5‰ level over the six hours run duration. We have not investigated how large this drift would have been without applying the detector voltage correction.

SIMS oxygen testing

We assessed the $\delta^{18}O$ heterogeneity of the three tourmaline materials with the Potsdam Cameca 1280-HR instrument. These analyses employed $^{133}Cs^{+}$ primary ion beam with a total impact energy of 20 keV and ~ 2.5 nA beam current focused to a *ca.* 5 µm diameter spot on the polished sample surface. Each analysis was preceded by a 2.5 nA, 60 s pre-sputtering in conjunction with a 20 µm raster. All analysis points were within 8 mm of the centre of the sample mount. Negative secondary ions were extracted using a -10 kV potential applied to the sample holder, with no offset voltage applied, in conjunction with a 40 eV wide energy window, which was mechanically centred at the beginning of the measurement session. Normal incidence, low energy electron flooding was used to suppress sample charging. Each analysis was preceded by an automatic centring routine for the instrument's field aperture in both X and Y and the centring of the beam on the contrast aperture in the Y direction only. A square 5000 × 5000 µm filed aperture, equivalent to a 50 × 50 µm field-of-view, a 400 µm contrast aperture, and a 114 µm wide entrance slit and a 500 µm wide exit slits were used for this fully automated data collection sequence. The instrument was operated in multi-collection Faraday cup mode using the instrument's NMR field stabilisation circuitry. The ion count rate on the $^{16}O^{-}$ peak was typically 2×10^{9} cps. Each analysis consisted of twenty integrations of 4 s duration each. Data were collected using a 10 µm × 10 µm primary beam raster, thereby assuring a flat bottom crater, for which the dynamic beam transfer option of the secondary ion optics was used to compensate. The analytical stability was monitored by interspersed measurements of the NIST SRM 610 silicate glass that was embedded in the same 1-inch diameter sample mount. Using this approach we detected an analytical drift amounting to 0.013‰ per hour over the course of the 16.6 h of continuous data acquisition. The analytical repeatability for the $n = 29$ determinations on the NIST SRM 610 glass drift monitor was ± 0.33‰ (1s), which improved to ± 0.21‰ after applying a linear drift correction (Table 4, Table S4). The analytical repeatability on all three of the Harvard tourmalines was similar to this value (Table 4), and hence we conclude that no major oxygen isotope heterogeneity is present in any of the three tourmaline RMs. The volume of a single crater that was produced under these conditions was determined to be 115 μm^3 using white light profilometry, including the pre-sputtering and beam centring processes, equivalent to a test portion mass of ~ 350 pg (based on a density of $\rho = 3.0$ g cm^{-3} for tourmaline).

Bulk sample isotope determinations

Solution MC-ICP-MS analysis of δ^7Li

Lithium isotope compositions were determined on acid-digested sample solutions by MC-ICP-MS in four laboratories: Woods Hole Oceanographic Institution, the University of Maryland, the University of Bristol, and the University of Bremen. The only information exchanged between the laboratories prior to analysis concerned the approximate Li mass fractions in the tourmalines and the need for a prolonged, high-pressure dissolution in order to achieve complete digestion. Each laboratory performed one or two independent dissolutions of separate aliquots of each RM, and in all but a few cases the separate dissolution samples were analysed between 2 and 5 times each. The analytical technique descriptions for each of the participating laboratories are given below, a summary of the results along with the final recommended values are shown in Table 5 and a compilation of all the data are given in Table S5. We note that the Li isotope analyses of elbaite #98144 at the University of Bristol were previously published by Ludwig *et al*. (2011). Independent of our study, Lin *et al*. (2019) reported Li isotope values for the Harvard schorl #112566 and elbaite #98144 analysed by solution ICP-MS. Their results are also shown on Table 5.

Woods Hole Oceanographic Institution: Multiple tourmaline fragments with a total mass between 1 and 10 mg were crushed and then digested in steel-clad PTFE bombs under pressure at 120 °C in a mixture of 1.5 ml HF and 0.5 ml concentrated HNO_3 for 2 days. The dried samples were taken up in 9 ml 1 mol l^{-1} HNO_3 with 80% methyl alcohol from which the Li fraction was separated by ion chromatography using a 10 ml AG 50W X8 (200–400 mesh) column (see Tomascak *et al.* 1999). The Li cuts were analysed with a Thermo-Finnigan NEPTUNE MC-ICP-MS using sample/calibrator bracketing with NIST SRM 8545 (see Rosner *et al.* 2007). The total Li blank of this procedure was < 0.5 ng, which is negligible for the elbaite and schorl materials and less than 1% of the Li recovered from an analysis of the dravite material. Since the isotopic composition of the blank can be assumed to be in the natural terrestrial range, we conclude that a 1% Li contribution from the blank does not significantly impact the determined δ^7Li values. The measurement repeatability precision ("within-run or internal" precision) of each $^7Li/^6Li$ measurement was < 0.1‰ (2SE). Multiple analysis of sample solutions for schorl and elbaite gave repeatabilities < 0.4‰ (2*s*, *n* = 4); the dravite solutions were measured only once. The δ^7Li values

from individual solution aliquots (schorl and dravite) deviated by less than 0.8‰ (Table 5). Rosner *et al.* (2007) estimated the trueness of the δ^7Li values from this procedure at *ca.* 0.5‰ or better based on concurrent analyses of independent RMs – NASS-5 from the North Atlantic and IAPSO from the Mid-Atlantic, as well as four basaltic to andesitic rock RMs (BHVO-1, BCR-2, JA-1 and JB-2).

University of Maryland: Tourmaline fragments having total masses ranging between 0.2 and 13.6 mg were lightly crushed and then cleaned for 15 min in an ultrasonic bath using high-purity (Milli-Q) water (18.2 MΩ cm resistivity). Two separate dissolution aliquots were obtained using the following procedure. Sample digestion took place in steel clad PTFE bombs at 160 °C under pressure in a 3:1 mixture of concentrated HF and concentrated HNO_3. The dried residua were refluxed with concentrated HNO_3, dried again and repeatedly refluxed with concentrated HCl until all fluorides were converted into chlorides and clear solutions were obtained. The final dried residua were taken up in 1 ml 4 mol l^{-1} HCl, and the Li fraction was separated by ion chromatography in columns loaded with Bio-Rad AG 50w-x12 (200–400 mesh) using the procedure described by Rudnick *et al*. (2004). Lithium loss during column chemistry was monitored by taking an additional 2 ml cut after the Li cut from each column. The total loss during this study was between 0.6% and 1.3% of the total Li in the sample, which does not affect the Li isotopic composition significantly (Marks *et al.* 2007). Lithium isotope analyses were made on a Nu-Plasma MC-ICP-MS instrument (for details see Teng *et al*. 2004). Each analysis was bracketed by measurements of a standard solution of the Li-carbonate RM NIST SRM 8545, and the ^{7}Li/^{6}Li value for the analysis was calculated relative to the average of the two bracketing runs. The total procedural blank during the course of the study was equivalent to a voltage of 4 mV for $^7Li^+$ ions. This compares with a voltage of 1–1.5 V obtained for a solution with 50 µg l^{-1} Li at a 40 µl min^{-1} uptake rate, resulting in a sample/blank ratio of ~ 300. The measurement repeatability precision ("internal or within-run precision") of ^{7}Li/^{6}Li measurements based on two blocks of twenty ratios each, was generally ≤ 0.2‰ (2*s*). The intermediate measurement precision of the method (over a period of NNN months), based on > 100 analyses of a purified NIST SRM 8545 standard solution, is ≤ 1.0‰ (2*s*, see Teng *et al.* 2004). Analytical trueness was monitored during each session by multiple measurements of two reference solutions: seawater IRMM-016 (Qi *et al*. 1997) and an in-house UMD-1 quality control material (a purified Li solution from Alfa Aesar®). The results for both reference solutions agree within uncertainties with previously published

values. Two measurements of the nepheline syenite RM STM-1 yielded +3.2 and +4.1‰, which are within the range of previously published values (Halama *et al.* 2008). The long-term bias of Li isotope measurements in the Maryland laboratory was monitored by multiple analyses of the BHVO-1 basalt RM, which gave 4.4‰ ± 0.7 (1SE), which is in good agreement with published values (4.3 to 5.8‰; James and Palmer 2000, Chan and Frey 2003, Bouman *et al.* 2004, Rudnick *et al.* 2004).

University of Bristol: The determinations on each of the three RMs were based on between 1 and 2 mg of material that was finely powdered, from which two separate aliquots were dissolved in the following three steps: first with a combined dissolution in a 2:6:1 ratio of concentrated HF-HNO_3-$HClO_4$ (where the perchloric acid is included to inhibit the formation of insoluble Li-fluorides, see Ryan and Langmuir 1987), followed by concentrated HNO_3 and then 6 mol l^{-1} HCl. The dissolution process incorporated repeated ultra-sonication. The dissolved samples were passed through two high aspect-ratio cation exchange columns (AG50W X12), using dilute HCl as eluant based on the approach of James and Palmer (2000), and described in detail by Marschall *et al*. (2007) and Pogge von Strandmann *et al*. (2011). The Li fractions were measured using a Thermo Finnegan Neptune MC-ICP-MS, with sample-bracketing using a solution of NIST SRM 8545 (Jeffcoate *et al*. 2004). Samples were analysed two or three times during the given sequence. The measurement repeatability precision ("internal or within-run precision") was typically better than ± 0.2‰ (2*s*). The intermediate measurement precision (i.e., over a long-term period of four years) for the Bristol laboratory was ≤ 0.3‰ (2*s*), based on analyses of silicate rock RMs BHVO-2 and BCR-2 (δ^7Li = 4.7 ± 0.2‰ *n* = 31 and δ^7Li = 2.6 ± 0.3‰ *n* = 18, respectively, all uncertainties 2*s*; Pogge von Strandmann *et al*. 2011).

University of Bremen: Values of δ^7Li of the three tourmaline materials were determined in the Isotope Geochemistry Laboratory at the MARUM - Center for Marine Environmental Sciences, University of Bremen. Sample digestion, separation and purification of lithium were modified after Moriguti and Nakamura (1998). Between 3 and 15 mg of crushed tourmaline sample were digested at 170 °C in 2 ml HF/HNO_3 mixture (5:1) in steel-clad PTFE bombs, dried at 80 °C, repeatedly re-dissolved in 2 ml of 2 mol l^{-1} HNO_3 and dried to convert all fluorides into nitrates. The decomposed samples were finally dissolved in 4 mol l^{-1} HCl. For the schorl and elbaite materials five solution aliquots per sample were taken, each containing between 60 and 220

ng Li; the Li-poor dravite sample could only be analysed once. Each aliquot solution went through a three-step purification procedure using BioRad® AG 50WX8 (200–400 mesh) resin. The first step removed the trivalent matrix elements (e.g. rare earth elements) using BioRad® Bio-Spin columns with 1 ml of the cation-exchange resin and 4 mol l^{-1} HCl (for conditioning the resin and loading the sample) and 2.8 mol l^{-1} HCl (to elute Li) as reagents. The second step removed the majority of matrix elements (e.g. Ca, Mg, etc.) using BioRad® Poly-Prep columns with 1.4 ml of the cation-exchange resin and 0.15 mol l^{-1} HCl as reagent. In the final step, Na was separated using BioRad® Bio-Spin columns with 1 ml resin and 0.15 mol l^{-1} HCl followed by 0.5 mol l^{-1} HCl in 50% ethanol as reagents. Lithium must be quantitatively separated from the sample matrix, since the loss of only 1% of Li during column separation as well as the presence of Na can result in significant shifts in the Li isotope composition (James and Palmer 2000, Nishio and Nakai 2002, Jeffcoate *et al*. 2004). Lithium loss during column separation was monitored by testing the collected head and tail fractions of each separation step. The total Li loss was typically < 0.1% of total collected Li, and was thus insignificant. Reference materials NIST SRM 8545 (LSVEC Li carbonate, Flesch *et al*. 1973), ZGI-TB-2 (clay shale), ZGI-GM (granite) and tourmaline IAEA-B-4 (powdered batch, Universität Bremen) were separated and analysed together with the samples as quality control materials. The Li blank input during the whole analytical procedure was less than 14 pg Li, which had no significant influence on the isotopic composition of the processed materials. Isotope analyses were performed on a MC-ICP-MS (Thermo Scientific Neptune Plus) using the stable introduction system together with a high-efficiency x-cone (Hansen *et al*. 2017). Processed samples and QCMs as well as the unprocessed NIST SRM 8545 were dissolved in 2% HNO_3, closely adjusted to 25 µg l^{-1} Li content and repeatedly analysed in the standard-sample bracketing mode using the unprocessed NIST SRM 8545 as calibrant. The 2% HNO_3 used for sample dissolution was measured as analytical baseline for correction. The determined Li isotope ratios are reported as delta-notation relative to NIST SRM 8545. The processed NIST SRM 8545 shows a δ^7Li value of -0.01 ± 0.11‰ (2*s*, *n* = 4) indicating that no significant isotope fractionation occurred during the measurement procedure, and confirming the long-term precision for the δ^7Li value of 0.01 ± 0.18‰ (2*s*, *n* = 78). δ^7Li values of ZGI-TB-2 (-3.4 ± 0.2‰, 2*s*, *n* = 2) agree well with published values of ZGI-TB (-3.3 ± 0.4‰, 2*s*; Romer *et al*. 2014). The ZGI-GM gives a δ^7Li value of -0.7 ± 0.1‰ (2*s*, *n* = 2), which fits well with the published value of -0.9 ± 0.6‰ (2*s*, *n* = 2) (Meixner *et al*. 2019). Tourmaline RM IAEA-B4 was also used as a quality control material, yielding a δ^7Li of 4.3 ± 0.3‰ (2*s*). Lin *et al*. (2019) reported a δ^7Li value of 5.64 for the B4

tourmaline; here we note that the value reported for schorl and elbaite in that manuscript are likewise higher than our values based on four independent laboratories. The "external" precision of silicate samples was generally ≤ 0.5‰ (2*s*). The repeatability of the individual δ^7Li values is reported as two standard deviations based on the five individually analysed sample aliquots.

Gas source analyses of oxygen isotopes

Oxygen isotope ratios were determined by gas-source mass spectrometry using either laser-fluorination or step-wise fluorination techniques in six independent laboratories: University of Wisconsin (Madison), the Open University (Milton Keynes), University of Göttingen, University of Cape Town, the Scottish Universities Environmental Research Centre SUERC (East Kilbride) and the National Environmental Isotope Facility of the British Geological Survey (Keyworth). Each laboratory analysed between one and four aliquots of grain fragments from each of the three tourmaline materials, and each analysis involved between one and four separate determinations. Additionally, all laboratories analysed the UWG-2 garnet RM (Valley *et al.* 1995) as a silicate traceability material. All laboratories reported δ^{18}O values; in addition, the Open University and University of Göttingen laboratories reported δ^{17}O results. Analytical technique descriptions for each of the participating laboratories are given below, a summary of the results is given in Table 6 and the compilation of all data is provided in Table S6. These tables also report the results obtained on the UWG-2 garnet traceability material; nearly all of the six participating gas source laboratories reported a mean value for UWG-2 which was in close agreement with the previously reported value of $\delta^{18}O_{SMOW}$ = 5.8 (Valley *et al*. 1995). Table 6 also shows the previously published δ^{18}O working values for the three Harvard tourmalines as reported by Dyar *et al*. (2001); for the dravite and elbaite materials good agreement is seen between these previous working values and the new results presented here. Finally, in Table 6 we also report Δ'^{17}O value for the Open University and Göttingen data sets, where Δ'^{17}O is defined as:

$$\Delta'^{17}O = 1000 \cdot \ln\left(\frac{\delta^{17}O}{1000} + 1\right) - 0.528 \cdot 1000 \cdot \ln\left(\frac{\delta^{18}O}{1000} + 1\right) \quad (4)$$

with both, δ^{17}O and δ^{18}O on VSMOW scale. To ensure that δ^{17}O is on the VSMOW scale, our data are linked via the composition of UWG-2 garnet, taken as Δ'^{17}O = -0.062‰, which is 0.01‰ lower than that of San Carlos olivine (Miller *et al*. 2020) that was measured relative to VSMOW2

and SLAP2 to be $\Delta'^{17}O$ = -0.052‰ (mean of the determinations by Pack *et al*. 2016, Sharp *et al*. 2016, Wostbrock *et al*. 2020).

University of Wisconsin: Oxygen isotope ratios were measured at the Department of Geoscience, University of Wisconsin-Madison. Aliquots of tourmaline weighing 1.9 to 3.3 mg were individually heated in a BrF_5 atmosphere using a CO_2 laser (λ = 10.6 μm) at a beam diameter of ~ 1 mm and a power of ~ 19 W. Evolved O_2 was cleaned cryogenically, converted to CO_2 on hot graphite, and analysed on mass stations 44, 45 and 46 using a Finnigan MAT 251 gas-source mass spectrometer. Values are reported in standard permil notation relative to VSMOW. The silicate RM UWG-2 (Valley *et al.* 1995) was analysed in the same measurement session as the tourmalines. UWG-2 is calibrated versus NBS-28 quartz ($\delta^{18}O$ = 9.59‰, Hut 1987). Analyses of the UWG-2 garnet on the same day of analysis yielded $\delta^{18}O$ = 5.76 ± 0.11‰ (2*s*, *n* = 4); tourmaline values were corrected by +0.04‰ to the published value of 5.80‰ for UWG-2, as recommended by Valley *et al.* (1995).

University of Cape Town: Aliquots of tourmaline grains between 1.8 to 4.3 mg were laser-heated in a reaction cell with BrF_5 (MIR 10-30 CO_2 laser, λ = 10.6 μm), with a spot diameter of 1 mm to 0.25 mm (start to finish, respectively) and between 1.5 and 15 W power. The released O_2 was purified in cold traps collected on 5 μm molecular sieve, and analysed offline as O_2 using a Thermo Delta XP mass spectrometer using the mass stations 32, 33 and 34. Raw data were initially recalculated to the VSMOW scale using the in-house reference Monastery garnet (Mon Gt; $\delta^{18}O$ = 5.38‰). Yields were calculated from inlet pressure to the mass spectrometer relative to that of Mon Gt, assuming a constant volume of the inlet system. The analyses were run on two separate sessions and yielded $\delta^{18}O$ values for the UWG-2 garnet of 5.67 and 5.69 and 5.81 and 5.87‰. Data were normalised to the accepted value for UWG-2 of 5.80‰ (Valley *et al.* 1995) and expressed in the permil notation relative to VSMOW. Full details of the method are given in Harris and Vogeli (2010).

University of Göttingen: Aliquots of tourmaline weighing ~ 2 mg were heated in a BrF_5 atmosphere by laser (λ = 10.6 μm). Evolved O_2 was cleaned cryogenically and by gas chromatography and was measured in a Thermo Finnigan Mat 253 gas source mass spectrometer

(for details see Pack *et al*. 2016). Values for $\delta^{17}O$ and $\delta^{18}O$ are reported in standard permil notation relative to VSMOW. The intermediate measurement precision (i.e., of a long-term period of NN months) (1*s*) was 0.04‰ for $\delta^{17}O$, 0.08‰ for $\delta^{18}O$, and 0.009‰ for $\Delta'^{17}O$ (note that the uncertainties for $\delta^{17}O$ and $\delta^{18}O$ are highly correlated; see also Wostbrock *et al*. 2020).

Open University (Milton Keynes): Aliquots of tourmaline weighing 2.0 to 2.1 mg were heated in a BrF_5 atmosphere by laser (λ = 10.6 μm) ramped up to ~ 15 W power. Evolved O_2 was prepared through a two-stage cryogenic purification process with an intermediate hot (110 °C) KBr reactor. The purified O_2 gas was cryofocused at the entrance of the analyser using zeolite molecular sieve at -196 °C before being analysed by gas-source mass spectrometer (Thermo Finnigan MAT 253). Details of analytical procedures are given in Miller *et al.* (1999). Values for $\delta^{17}O$ and $\delta^{18}O$ are reported in conventional ‰ notation relative to VSMOW. Typical intermediate measurement precision (i.e., over a period of NN months) was ± 0.052‰ for $\delta^{17}O$; ± 0.093‰ for $\delta^{18}O$; ± 0.017‰ for $\Delta'^{17}O$ (2*s*) (Greenwood *et al.* 2015). Analyses of UWG-2 yielded 5.75± 0.06‰ (1*s*, *n* = 4).

SUERC East Kilbride: Aliquots of tourmaline weighing between 1.7 to 2.9 milligrams of tourmaline, and between 1.4 and 3.0 milligrams of UWG-2 garnet, were pre-fluorinated overnight, under vacuum in the sample chamber. Samples were then individually heated in a ClF_3 atmosphere by laser (SYNRAD J48-2 CO_2 laser λ = 10.6 μm), following the method of Sharp (1990). The evolved O_2 was cleaned cryogenically, and passed through an on-line hot mercury diffusion pump, before being converted to CO_2 on hot graphite, and analysed by gas-source mass spectrometer (VG SIRA2). Values are reported in conventional permil notation relative to VSMOW. Analyses of the UWG-2 garnet during the measurement session yielded 5.75 ± 0.08‰ (1*s*, *n* = 9). Values were corrected by 0.04‰ to the accepted value of 5.80 for UWG-2 (Valley *et al*. 1995).

BGS (Keyworth): The tourmalines, weighing between 6.1 and 6.6 mg, were powdered, transferred to pure nickel reaction vessels, and furnace-heated to 700 °C in an excess of BrF_5 for an extended period (> 16 h). The evolved O_2 was cleaned cryogenically, converted to CO_2 on hot graphite, and collected under liquid N_2. Oxygen isotope analyses were conducted with a Thermo Finnigan MAT 253 dual inlet mass spectrometer. Values are reported in standard δ-notation in

permil relative to VSMOW calibrated using NBS28 quartz, which has an assigned composition of $\delta^{18}O = 9.59‰$ (Hut 1987). Analyses of the UWG-2 garnet during the session yielded 5.49 ± 0.46‰ (1*s*, *n* = 3). Values were corrected by 0.31‰ to the accepted value of 5.80‰ for UWG-2 (Valley *et al*. 1995). It is noted that the Keyworth laboratory does not normally run high temperature minerals, and fluorination was conducted at a temperature well above the typical 500 °C used in this facility for biogenic silica. This deviation for the Keyworth validated operating protocol may have contributed to the somewhat lower mean $\delta^{18}O$ value (-0.3‰; *n* = 3) determined on the UWG-2 garnet traceability material.

Discussion

Table 7 summarises the best available values for stable isotope ratios of the three Harvard tourmaline materials.

Major element compositions

With respect to the major element compositions of the three Harvard tourmaline RMs, we believe the best estimates of their major element compositions and their inter-fragment variabilities are provided by the grand means of two EPMA data sets presented in Table 1. In general, the grand means reported from Potsdam and Madison agree well, though biases outside the reported repeatability are also visible for some elements. Both sets of EPMA results provide data that characterise the composition of the tourmalines. We note that the values for B composition determined by EPMA are in excellent agreement with earlier non-EPMA technique data (Dyar *et al.* 2001). However, due to different analytical EPMA protocols further examinations of all three tourmaline RMs will be necessary in order to establish recommended values. For the time being, the grand means reported in Table 1 should be considered as working values, subject to possible future refinement.

Working values for lithium mass fractions

Based on the observed repeatabilities of our SIMS data as compared with both the (presumably) homogeneous NIST SRM 610 silicate glass and the "within-run" precision of the individual SIMS

measurements (Table 2), it appears that significant variability in the Li_2O contents are present in all three materials. Furthermore, our "current best estimate" values for Li contents (Table 7) are derived from a SIMS calibration based on the NIST SRM 610 glass; as such, we do not have a matrix-matched calibration. We conclude that the Li content values presented in Table 7 should only be used as rough indicators, and that any values calibrated using these materials should employ multiple grains so as to suppress issues related to the observed sample heterogeneity.

Recommended values for lithium isotopes

A comparison of the δ^7Li values determined by the four laboratories (Table 5) shows good agreement for all three RMs, the only noteworthy observation being the consistently lower δ^7Li values reported in the University of Maryland data set, which differs by roughly 1‰ from the results reported by Bremen, Bristol and Woods Hole. The source of this phenomenon is unclear, particularly in view of the detailed quality assurance plans implemented by all four bulk analyses laboratories. In total there are eight repeated pairs of data in our full data set (Table 5), and these have on average a difference of only 0.38‰ between the members of the pairs. Equally, the overall repeatabilities of the SIMS homogeneity assessments were better than ± 0.8‰ (1*s*) for both of the Li-rich materials (Table 3). Hence, both the repeatability of our analytical methods and the homogeneity observed by SIMS are significantly better than the observed spread in the result. Based on these observations, we suggest that the median δ^7Li values based on the individual (n = 6 or 7) bulk δ^7Li determinations represent the best possible estimates of the true value of the three materials. These are reported in Table 5 and their assigned uncertainties are the repeatabilities of the complete set of determinations divided by $\sqrt{(n - 1)}$. We note that our results for schorl and elbaite are roughly 0.9‰ lower than those reported by Lin *et al*. (2019) (see Table 5).

Recommended values for oxygen isotopes

The results of thirty-three $\delta^{18}O$ laser and step-wise fluorination determinations reported by six independent laboratories show excellent agreement for all three of the tourmaline RMs **(**Table 6**).** The "within-run" precision of individual analyses was better than ± 0.1‰ (1*s*) for all of the gas source data (Table S6). With regard to the homogeneity at the picogram sampling scale, our SIMS data (Table 4) yielded repeatabilities similar to those obtained on the NIST SRM 610 silicate glass, which we presume to be isotopically homogeneous at the SIMS sampling scale. We therefore conclude that the recommended $\delta^{18}O$ values reported in Table 7 can be used to calibrate

in situ oxygen isotope ratio measurements at ± 0.3‰ (1*s*) data quality or better. Finally, we note that the new data are in good agreement with the $\delta^{18}O$ values for dravite and elbaite reported in Dyar *et al.* (2001) whereas in the case of schorl there is a difference of 0.66‰ between our gas-source data mean and that from the earlier publication (see Table 6). As our data are based on multiple results reported by six independent laboratories, we recommend that the $\delta^{18}O$ and $\delta^{17}O$ and $\Delta'^{17}O$ values reported in Table 7 should be used for calibrating future studies.

SIMS matrix effects

In the case of the three Harvard tourmaline RMs it is not possible for us to say anything with regards to SIMS matrix effects related to Li mass fraction determinations as we do not have any independently determined value for the three materials in which we have high confidence. Equally, in the case of $^{7}Li/^{6}Li$ determinations we cannot conclude anything meaningful regarding a chemical matrix effect. The large differences in Li mass fractions mean that each of the three RMs had to be run under distinct analytical conditions, preventing any direct comparison. The only thing that can be said concerning a matrix effect is through comparing the schorl RM and the concurrently run NIST SRM 610 silicate glass, which was used as a drift monitor. Kasemann *et al.* (2005) published a solution MC-ICP-MS value of $\delta^{7}Li_{L\text{-}SVEC} = 32.50 \pm 0.02$ for NIST SRM 610, which is equivalent to an absolute isotope ratio of $^{7}Li/^{6}Li = 12.5686$ (see Equation 3). During our homogeneity testing we obtained on $n = 8$ measurements $^{7}Li^{+}/^{6}Li^{+} = 11.8166$ for NIST SRM 610 (Table 3), corresponding to an Instrumental Mass Fractionation (IMF) of 11.8166/12.5686 = 0.94016. For the concurrently analysed schorl, the IMF value is 0.94993, based on our recommended $\delta^{7}Li = 5.52$ (Table 7) and the observed average $^{7}Li^{+}/^{6}Li^{+} = 11.6273$ (Table 3). Comparison of these IMF values indicates a difference of *circa* 10‰ between the schorl and silicate glass matrix. Similar to what has already been demonstrated for SIMS boron isotope data (e.g., Rosner *et al*. 2008), the use of NIST silicate glass RMs (SRM 61x series) for calibrating SIMS lithium isotope measurements of tourmaline leads to a grossly biased result.

During our SIMS $^{18}O/^{16}O$ homogeneity test run we ran all three of the Harvard tourmaline RMs as well as NIST SRM 610 glass (as drift monitor) during a single analytical sequence under identical analytical conditions. This allows us to evaluate the impact of the various matrices on the SIMS IMF value. For the tourmaline RMs we used the grand mean $\delta^{18}O$ values reported in Table 6 in conjunction with the absolute ratio for SMOW of $^{18}O/^{16}O = 0.00200520$ (Baertschi 1976). In

the case of NIST SRM 610 silicate glass we used the value reported by Kasemann *et al*. (2001) of $\delta^{18}O_{SMOW} = 10.91$ (see Equation (1) for conversion to absolute isotope ratio). The resulting IMF values for each of these four materials are reported in Table 4. Among the three tourmaline RMs the maximum difference in IMF is 1.9‰, as seen between schorl and elbaite, with dravite yielding an IMF intermediate between the two. These differences in IMF are large compared with the analytical uncertainties and are similar to variations in IMF reported for oxygen isotope ratio determinations on tourmaline by Marger *et al*. (2019); that earlier work reported that tourmalines having low iron contents (e.g., elbaite) tend to measure comparatively high $^{18}O^-/^{16}O^-$ SIMS results. This observation suggests that, despite the low uncertainties of the gas-source data and the good repeatability of our SIMS method, the determination of $\delta^{18}O$ in natural tourmalines at precision levels better than 0.5‰ will be difficult except where there is a close chemical match between the unknown sample and one of these RMs, as has been shown for garnet and other minerals (Valley and Kita 2009, Page *et al*. 2010). For the case of NIST SRM 610, the IMF was biased by between 3‰ and 5‰ relative to the dravite and schorl RMs, respectively. This confirms that, at least in the case of SIMS, the use of a silicate glass calibrant is inappropriate for $\delta^{18}O$ determinations on tourmaline.

Material availability

Since 2014 the three Harvard tourmalines RMs described here have been distributed through IAGeo Limited (www.iageo.com), and it is expected this arrangement will continue on into the future. Vials containing ca. 100 mg of tourmaline (samples HMGM #98144.1, HMGM # 112566.1 and HMGM #108796.1) are therefore readily available to the global user community. In light of the large number of splits that were produced of each of these materials (128 or 512 units) in conjunction with past levels of demand, it is reasonable to expect this resource will last for at least two decades into the future.

Data availability statement

Acknowledgements

MW and RT acknowledge F. Couffignal for his skills at operating the SIMS instrument and U. Dittmann for excellent SIMS sample preparation work (Potsdam). CH thanks Sherissa Roopnarain (Cape Town) for help with mass spectrometry. RH acknowledges the support and advice of R. Rudnick, W.F. McDonough and R. Ash in the Maryland laboratory. R. Przybilla and D. Kohl (University of Göttingen) are thanked for preparing and analysing the samples and keeping the laboratory running. JWV and MJS (University of Wisconsin) are supported by the U.S. National Science Foundation (EAR-1524336) and Department of Energy (DE-FG02-93-ER14389). MR acknowledges the use of the NSF-supported WHOI ICP-MS facility and thanks Larry Ball and Jerzy Blusztajn for their assistance. Analyses at Bristol were supported by NERC grant NER/C510983/1. We also thank two reviewers who provided valuable suggestions for improving this manuscript. Finally, we wish to thank the Harvard Museum for on-going support of such projects.

References

Armstrong J.T. (1995)
CITZAF: A package of correction programs for the quantitative electron microbeam X-ray analysis of thick polished materials, thin films, and particles. **Microbeam Analysis, 4**, 177–200.

Baertschi P. (1976)
Absolute ^{18}O content of Standard Mean Ocean Water. **Earth and Planetary Science Letters, 31**, 341–344.

Barkan E. and Luz B. (2005)
High precision measurements of $^{17}O/^{16}O$ and $^{18}O/^{16}O$ ratios in H_2O. **Rapid Communications in Mass Spectrometry 19**, 3737–3742.

Bell D.R., Hervig R.L., Buseck P.R. and Aulbach S. (2009)
Lithium isotope analysis of olivine by SIMS: Calibration of a matrix effect and application to magmatic phenocrysts. **Chemical Geology, 258**, 5–16.

Bouman C., Elliott T. and Vroon P.Z. (2004)
Lithium inputs to subduction zones. **Chemical Geology, 212**, 59–79.

Brand W.A., Coplen T.B., Vogl J., Rosner M. and Prohaska T. (2014)
Assessment of international reference materials for isotope-ratio analysis (IUPAC Technical Report). **Pure and Applied Chemistry, 86,** 425–467.

Chan L.-H. and Frey F.A. (2003)
Lithium isotope geochemistry of the Hawaiian plume: results from the Hawaii Scientific Drilling Project and Koolau Volcano. **Geochemistry, Geophysics, Geosystems, 4**, 8707.

Coplen T.B. (2011)
Report of stable isotopic composition Reference Material LSVEC (carbon and lithium isotopes in lithium carbonate). **United States Geological Survey Reston Stable Isotope Laboratory**, 3pp.

Dyar M.D., Wiedenbeck M., Robertson D., Cross L.R., Delaney J.S., Ferguson K., Francis C.A., Grew E.S., Guidotti C.V., Hervig R.L., Hughes J.M., Husler J., Leeman W., McGuire A.V., Rhede D., Rothe H., Paul R.L., Richards I. and Yates M. (2001)
Reference minerals for microanalysis of light elements. **Geostandards Newsletter: The Journal of Geostandards and Geoanalysis, 25**, 441–463.

Flesch G.D., Anderson A.R. and Svec H.J. (1973)
A secondary isotopic standard for $^{6}Li/^{7}Li$ determinations. **International Journal of Mass Spectrometry and Ion Physics, 12**, 265–272.

Frondel C., Biedl A. and Ito J. (1966)
New type of ferric iron tourmaline. **American Mineralogist, 51**, 1501–1505.

Gonfiantini R., Tonarini S., Gröning M., Adorni-Braccesi A., Al-Ammar A.S., Astner M., Bächler S., Barnes R.M., Bassett R.L., Cocherie A., Deyhle A., Dini A., Ferrara G., Gaillardet J., Grimm J., Guerrot C., Krähenbühl U., Layne G., Lemarchand D., Meixner A., Northington D.J., Pennisi M., Reitznerová E., Rodushkin I., Sugiura N., Surberg R., Tonn S., Wiedenbeck M., Wunderli S., Xiao Y. and Zack T. (2003)
Intercomparison of boron isotope and concentration measurements. Part II: Evaluation of results. **Geostandards Newsletter: The Journal of Geostandards and Geoanalysis, 27**, 41–57.

Greenwood R.C., Barrat J.-A., Scott E.R.D., Haack H., Buchanan P.C., Franchi I.A., Yamaguchi A., Johnson D., Bevan A.W.R. and Burbine T.H. (2015)
Geochemistry and oxygen isotope composition of main-group pallasites and olivine-rich clasts in mesosiderites: Implications for the 'Great Dunite Shortage' and HED-mesosiderite connection. **Geochimica et Cosmochimica Acta, 169**, 115–136.

Halama R., McDonough W.F., Rudnick R.L. and Bell K. (2008)
Tracking the lithium isotopic evolution of the mantle using carbonatites. **Earth and Planetary Science Letters, 265**, 726–742.

Hansen C.T., Meixner A., Kasemann S.A. and Bach W. (2017)
New insight on Li and B isotope fractionation during serpentinization derived from batch reaction investigations. **Geochimica et Cosmochimica Acta, 217**, 51–79.

Harms A.V. and Assonov A. (2018)
Reference sheet reference material LSVEC (Li-carbonate) Reference Material for Li-isotope ratio. **International Atomic Energy Agency**, 5pp.

Harris C. and Vogeli J. (2010)
Oxygen isotope composition of garnet in the Peninsula Granite, Cape Granite Suite, South Africa: Constraints on melting and emplacement mechanisms. **South African Journal of Geology, 113**, 401–412.

Henry D.J., Novák M., Hawthorne F.C., Ertl A., Dutrow B.L., Uher P. and Pezzotta F. (2011)
Nomenclature of the tourmaline supergroup minerals. **American Mineralogist, 96**, 895–913.

Herwartz D., Pack A., Krylov D., Xiao Y., Muehlenbachs K., Sengupta S. and Di Rocco T. (2015)
Revealing the climate of 'snowball Earth' from $\Delta^{17}O$ systematics of hydrothermal rocks. **Proceedings of the National Academy of Sciences, 112**, 5337–5341.

Hut G. (1987)
Consultants' group meeting on stable isotope reference samples for geochemical and hydrological investigations. **International Atomic Energy Agency (Vienna)**, 49pp.

Hutchinson R.W. and Claus R.J. (1956)
Pegmatite deposits, Alto Ligonha, Portuguese East Africa. **Economic Geology, 51**, 575–780.

James R.H. and Palmer M.R. (2000)
The lithium isotope composition of international rock standards. **Chemical Geology, 166**, 319–326.

Jeffcoate A.B., Elliott T., Thomas A. and Bouman C. (2004)
Precise, small sample size determinations of lithium isotopic compositions of geological reference materials and modern seawater by MC-ICP-MS. **Geostandards and Geoanalytical Research, 28**, 161–172.

Jochum K.-P., Weis U., Stoll B., Kuzmin D., Yang Q., Raczek I., Jakob D.E., Stracke A., Birbaum K., Frick D.A., Guenther D. and Enzweiler J. (2011)
Determination of reference values for NIST SRM 610–617 glasses following ISO guidelines. **Geostandards and Geoanalytical Research, 35**, 397–429.

Kasemann S., Meixner A., Rocholl A., Vennemann T., Rosner M., Schmitt A.K. and Wiedenbeck M. (2001)

Boron and oxygen isotope composition of certified reference materials NIST SRM 610/612 and reference materials JB-2 and JR-2. **Geostandards Newsletter: The Journal of Geostandards and Geoanalysis, 25**, 405–416.

Kasemann S.A., Jeffcoate A.B. and Elliott T. (2005)
Lithium isotope composition of basalt glass reference material. **Analytical Chemistry, 77**, 5251–5257.

Kutzschbach M., Wunder B., Trumbull R.B., Rocholl A., Meixner A. and Heinrich W. (2017)
An experimental approach to quantify the effect of tetrahedral boron in tourmaline on the boron isotope fractionation between tourmaline and fluid. **American Mineralogist, 102**, 2505–2511.

Leeman W.P. and Tonarini S. (2001)
Boron isotopic analysis of proposed borosilicate mineral reference samples. **Geostandards Newsletter: The Journal of Geostandards and Geoanalysis, 25**, 441–403.

Li W., Ni B., Jin D. and Zhang Q. (1988)
Measurement of the absolute abundance of oxygen-17 in V-SMOW. **Chinese Science Bulletin, English Translation, 33**, 1610–1613.

Lin J., Liu Y., Hu Z., Chen W., Zhang C., Zhao K. and Jin X. (2019)
Accurate analysis of Li isotopes in tourmalines by LA-MC-ICP-MS under "wet" conditions with non-matrix-matched calibration. **Journal of Analytical Atomic Spectrometry, 34**, 1145–1153.

Ludwig T., Marschall H.R., Pogge von Strandmann P.A.E., Shabaga B.M., Fayek M. and Hawthorne F.C. (2011)
A secondary ion mass spectrometry (SIMS) re-evaluation of B and Li isotopic compositions of Cu-bearing elbaite from three global localities. **Mineralogical Magazine, 75**, 2485–2494.

Marger K., Luisier C., Baumgartner L.P., Putlitz B., Dutrow B.L., Bouvier A.-S. and Dini A. (2019)

Origin of Monte Rosa whiteschist from *in-situ* tourmaline and quartz oxygen isotope analysis by SIMS using new tourmaline reference materials. **American Mineralogist, 104**, 1503–1520.

Marger K., Harlaux M., Rielli A., Baumgartner L.P., Dini A., Dutrow B.L. and Bouvier A.-S. (2020)
Development and re-evaluation of tourmaline reference materials for *in situ* measurement of boron δ values by secondary ion mass spectrometry. **Geostandards and Geoanalytical Research, 44**, 593–615.

Marks M.A.W., Rudnick R.L., McCammon C., Vennemann T. and Markl G. (2007)
Arrested kinetic Li isotope fractionation at the margin of the Ilímaussaq complex, South Greenland: Evidence for open-system processes during final cooling of Peralkaline igneous rocks. **Chemical Geology, 246**, 207–230.

Marschall H.R. and Jiang S.-Y. (2011)
Tourmaline isotopes: No element left behind. **Elements, 7**, 313–319.

Marschall H.R. and Foster G.L. (2018)
Boron isotopes – The fifth element. **Advances in Geochemistry, 7**, 249–272.

Marschall H.R., Pogge von Strandmann P.A.E., Seitz H.-M., Elliott T. and Niu Y. (2007)
The lithium isotopic composition of orogenic eclogites and deep subducted slaboratories. **Earth and Planetary Science Letters, 262**, 563–580.

Matthews A., Putlitz B., Hamiel Y. and Hervig R.L. (2003)
Volatile transport during the crystallization of anatectic melts: Oxygen, boron and hydrogen stable isotope study on the metamorphic complex of Naxos, Greece. **Geochimica et Cosmochimica Acta, 67**, 3145–3163.

Meixner A., Sarchi C., Lucassen F., Becchio R., Caffe P.J., Lindsay J., Rosner M. and Kasemann S.A. (2019)

Lithium concentrations and isotope signatures of Palaeozoic basement rocks and Cenozoic volcanic rocks from the Central Andean arc and back-arc. **Mineralium Deposita, 55**, 1071–1084.

Míková J., Košler J. and Wiedenbeck M. (2014)
Matrix effects during laser ablation MC-ICP-MS analysis of boron isotopes in tourmaline. **Journal of Analytical and Atomic Spectrometry, 29**, 903–914.

Miller M.F., Franchi I.A., Sexton A. and Pillinger C.T. (1999)
High precision $\Delta^{17}O$ isotope measurements of oxygen from silicates and other oxides: Method and applications. **Rapid Communications in Mass Spectrometry, 13**, 1211–1217.

Miller M.F., Pack A., Bindeman I.N. and Greenwood R.C. (2020)
Standardizing the reporting of $\Delta'^{17}O$ data from high precision oxygen triple-isotope ratio measurements of silicate rocks and minerals. **Chemical Geology, 532**, 119332.

Moriguti T. and Nakamura E. (1998)
Across-arc variation of Li isotopes in lavas and implications for crust/mantle recycling at subduction zones. **Earth and Planetary Science Letters, 163**, 167–174.

Nishio Y. and Nakai S. (2002)
Accurate and precise lithium isotopic determinations of igneous rock samples using multi-collector inductively coupled plasma-mass spectrometry. **Analytica Chimica Acta, 456**, 271–281.

Pack A. and Herwartz D. (2014)
The triple oxygen isotope composition of the Earth mantle and understanding $\Delta^{17}O$ variations in terrestrial rocks and minerals. **Earth and Planetary Science Letters 390**, 138–145.

Pack A., Tanaka R., Hering M., Sengupta S., Peters S. and Nakamura E. (2016)
The oxygen isotope composition of San Carlos olivine on the VSMOW2-SLAP2 scale. **Rapid Communications in Mass Spectrometry, 30**, 1495–1504.

Page F.Z., Kita N.T. and Valley J.W. (2010)

Ion microprobe analysis of oxygen isotopes in garnets of complex chemistry. **Chemical Geology, 270**, 9–19.

Pogge von Strandmann P.A.E., Elliott T., Marschall H.R., Coath C., Lai Y.-J., Jeffcoate A.B. and Ionov D.A. (2011)
Variations of Li and Mg isotope ratios in bulk chondrites and mantle xenoliths. **Geochimica et Cosmochimica Acta, 75**, 5247–5268.

Qi H.P., Taylor P.D.P, Berglund M. and de Bièvre P. (1997)
Calibrated measurements of the isotopic and atomic weight of the natural Li isotopic reference material IRMM-016. **International Journal of Mass Spectrometry and Ion Processes, 171**, 263–268.

Romer R.L., Meixner A. and Hahne K. (2014)
Lithium and boron isotopic composition of sedimentary rocks – The role of source history and depositional environment. A 250 Ma record from the Cadomian orogeny to the Variscan orogeny. **Gondwana Research, 26**, 1093–1110.

Rosner M., Ball L., Peucker-Ehrenbrink B., Blusztajn J., Bach W. and Erzinger J. (2007)
A simplified, accurate and fast method for Li isotope analysis of rocks and fluids, and δ^7Li values of seawater and rock reference materials. **Geostandards and Geoanalytical Research, 31**, 77–88.

Rosner M., Wiedenbeck M. and Ludwig T. (2008)
Composition-induced variations in SIMS instrumental mass fractionation during boron isotope ratio measurements of silicate glasses. **Geostandards and Geoanalytical Research, 32**, 27–38.

Rudnick R.L., Tomascak P.B., Heather B.N. and Gardner L.R. (2004)
Extreme lithium isotopic fractionation during continental weathering revealed in saprolites from South Carolina. **Chemical Geology, 212**, 45–57.

Ryan J.G. and Langmuir C.H. (1987)

The systematics of lithium abundances in young volcanic rocks. **Geochimica et Cosmochimica Acta, 51**, 1727–1741.

Sharp Z.D. (1990)
A laser-based microanalytical method for the *in-situ* determination of oxygen isotope ratios of silicates and oxides. **Geochimica et Cosmochimica Acta, 54**, 1353–1357.

Sharp Z.D., Gibbons J.A., Maltsev O., Atudorei V., Pack A., Sengupta S., Shock E.L. and Knauth L.P. (2016)
A calibration of the triple oxygen isotope fractionation in the SiO_2-H_2O system and applications to natural samples. **Geochimica et Cosmochimica Acta, 186**, 105–119.

Siegel K., Wagner T., Trumbull R.B., Jonsson E., Matalin G., Wälle M. and Heinrich C.A. (2016)
Stable isotope (B,H,O) and mineral-chemistry constraints on the magmatic to hydrothermal evolution of the Varutrask rare-element pegmatite (northern Sweden). **Chemical Geology, 421**, 1–16.

Slack J.F. and Trumbull R.B. (2011)
Tourmaline as a recorder of ore-forming processes. **Elements, 7**, 321–326.

Taylor B.E., Palmer M.R. and Slack J.F. (1999)
Mineralizing fluids in the Kidd Creek massive sulfide deposit, Ontario: Evidence from oxygen, hydrogen, and boron isotopes in tourmaline. **Economic Geology, Monograph 10**, 389–414.

Teng F.-Z., McDonough W.F., Rudnick R.L., Dalpé C., Tomascak P.B., Chappell B.W. and Gao S. (2004)
Lithium isotopic composition and concentration of the upper continental crust. **Geochimica et Cosmochimica Acta, 68**, 4167–4178.

Tomascak P.B. (2004)

Developments in the understanding and application of lithium isotopes in the Earth and planetary sciences **In: Johnson C.M., Beard B.A. and Albarède F. (eds), Geochemistry of non-traditional stable isotopes. Reviews in Mineralogy and Geochemistry 55**, 153–195.

Tomascak P.B., Carlson R.W. and Shirey S.B. (1999)
Accurate and precise determination of Li isotopic compositions by multi-collector sector ICP-MS. **Chemical Geology, 158**, 145–154.

Tomascak P.B., Magna T. and Dohmen R. (2016)
Advances in lithium isotope geochemistry. **Advances in Geochemistry 7. Springer (Heidelberg)**, 195pp.

Tonarini S., Pennisi M., Adorni-Braccesi A., Dini A., Ferrara G., Gonfiantini R., Wiedenbeck M. and Gröning M. (2003)
Intercomparison of boron isotope concentration measurements. Part I: Selection, preparation and homogeneity tests of the intercomparison materials. **Geostandards Newsletter: The Journal of Geostandards and Geoanalysis, 27**, 21–39.

Valley J.W. (2003)
Oxygen isotopes in zircon. **Reviews in Mineralogy, 53**, 343–385.

Valley J.W. and Cole D. (editors) (2001)
Stable isotope geochemistry. **Reviews in Mineralogy, 43**, 531pp.

Valley J.W., Kita N.T. (2009)
In situ oxygen isotope geochemistry by ion microprobe. In: Fayek M. (ed.), Secondary ion mass spectrometry in the Earth sciences. **MAC Short Course, 41**, 19–63.

Valley J.W., Kitchen N., Kohn M.J., Niendorf C.R. and Spicuzza J.J. (1995)
UWG-2, a garnet standard for oxygen isotope ratios: Strategies for high precision and accuracy with laser heating. **Geochimica et Cosmochimica Acta, 59**, 5223–5231.

Wostbrock J.A., Cano E.J. and Sharp Z.D. (2020)
An internally consistent triple oxygen isotope calibration of standards for silicates, carbonates and air relative to VSMOW2 and SLAP2. **Chemical Geology, 533**, 119432.

Supporting information

The following supporting information may be found in the online version of this article:

Table S1. Measurement results for tourmaline reference materials by electron probe microanalysis, complete data set.
Table S2. Lithium mass fraction homogeneity test results by SIMS, complete data set.
Table S3. Lithium isotope homogeneity tests by SIMS, complete data set.
Table S4. Oxygen isotope homogeneity test by SIMS, complete data set.
Table S5. Wet chemical lithium isotope ratio measurement results, complete data set.
Table S6. Gas source oxygen isotope ratio measurement results.

This material is available from: http://onlinelibrary.wiley.com/doi/10.1111/ggr.00000/abstract (This link will take you to the article abstract).

Figure caption

Figure 1. Al-Fe-Mg diagram (molar proportions) showing the composition of the three Harvard tourmaline RMs investigated by this study (see Table 1). The positions of some of the more common tourmaline end members as well as that of the "B4" tourmaline RM (Tonarini *et al.* 2003) are also indicated. We point the reader to Marger *et al*. (2019, 2020) for other recent efforts to characterise alternative tourmaline isotope calibration materials.

Table 1: Major element compositions based on EPMA.
Table 2: Summary of SIMS homogeneity tests for lithium mass fraction and new working values.
Table 3: Summary of SIMS homogeneity tests for lithium isotope ratios.
Table 4: Summary of SIMS homogeneity tests for oxygen isotope ratios.
Table 5: Summary of results of $\delta^7Li_{L\text{-}SVEC}$ by solution ICP mass spectrometry.
Table 6: Summary results of oxygen-isotope analyses by gas source mass spectrometry.
Table 7: Compilation of reference values for the three Harvard tourmaline materials.

Table 1.
Summary results of homogeneity tests by electron probe microanalysis

SCHORL 112566.1		SiO_2	TiO_2	Al_2O_3	FeO	MnO	MgO	CaO	Na_2O	K_2O	B_2O_3	ZnO	Li_2O	F	OH	-O 2 = 2F-	Total (% *m/m*)
	Potsdam																
Fragment 1	mean	32.20	0.66	32.01	14.87	1.05	0.19	0.16	2.12	0.05	10.04	nd	nd	nd	nd	–	93.34
	1*s* (*n* = 4)	0.29	0.05	0.13	0.32	0.22	0.03	0.03	0.08	0.02	0.44						
Fragment 5	mean	32.34	0.51	32.20	14.72	1.06	0.23	0.17	2.10	0.03	10.10	nd	nd	nd	nd	–	93.45
	1*s* (*n* = 4)	0.25	0.02	0.11	0.50	0.07	0.03	0.02	0.07	0.03	0.49						
Fragment 9	mean	32.50	0.65	31.85	14.15	1.03	0.18	0.16	2.06	0.04	10.17	nd	nd	nd	nd	–	92.79
	1*s* (*n* = 4)	0.31	0.06	0.35	0.76	0.09	0.02	0.03	0.07	0.03	0.28						
Fragment 12	mean	32.51	0.49	32.08	14.60	1.07	0.22	0.14	2.12	0.04	10.37	nd	nd	nd	nd	–	93.64
	1*s* (*n* = 4)	0.59	0.07	0.18	0.50	0.18	0.03	0.03	0.06	0.03	0.22						
Fragment 14	mean	32.48	0.68	31.61	14.99	0.88	0.26	0.13	2.12	0.05	10.01	nd	nd	nd	nd	–	93.21
	1*s* (*n* = 4)	0.56	0.07	0.17	0.38	0.07	0.02	0.05	0.05	0.02	0.26						
Fragment 15	mean	32.28	0.66	32.01	14.13	1.18	0.18	0.13	2.16	0.06	10.04	nd	nd	nd	nd	–	92.83
	1*s* (*n* = 4)	0.37	0.09	0.32	0.33	0.16	0.04	0.06	0.05	0.02	0.22						
Schorl grand mean		**32.37**	**0.63**	**31.99**	**14.55**	**1.02**	**0.21**	**0.15**	**2.13**	**0.04**	**10.11**						**93.21**
	1*s* (*n* = 24)	0.44	0.10	0.30	0.60	0.17	0.04	0.04	0.07	0.03	0.37						
	1*s* (%)	1.37	16.73	0.95	4.15	16.62	19.88	27.93	3.38	59.97	3.62						
	Madison																
Fragment 1	mean	33.43	0.54	34.33	15.05	1.13	0.22	0.15	2.01	0.03	9.23	0.25	0.12	0.39	1.89	0.16	98.59
	1*s* (*n* = 4)	0.06	0.02	0.13	0.08	0.06	0.01	0.01	0.07	0.01	0.64	0.06		0.02	0.55		
Fragment 2	mean	33.23	0.54	34.42	14.63	1.23	0.21	0.14	2.03	0.05	9.30	0.32	0.12	0.44	1.49	0.18	97.96
	1*s* (*n* = 4)	0.15	0.02	0.11	0.15	0.06	0.01	0.01	0.06	0.01	0.42	0.05		0.02	0.44		
Fragment 3	mean	33.35	0.57	33.74	15.52	1.17	0.29	0.17	2.06	0.04	10.01	0.24	0.12	0.48	1.17	0.20	98.73
	1*s* (*n* = 4)	0.22	0.06	1.52	1.59	0.22	0.19	0.05	0.16	0.01	0.43	0.06		0.10	0.13		
Fragment 4	mean	33.42	0.52	34.19	14.85	1.19	0.19	0.13	2.02	0.04	9.77	0.28	0.12	0.39	1.51	0.17	98.46
	1*s* (*n* = 4)	0.14	0.02	0.16	0.13	0.08	0.02	0.02	0.04	0.00	0.46	0.07		0.02	0.55		
Fragment 5	mean	32.84	0.57	34.29	14.57	1.22	0.20	0.13	1.97	0.04	10.17	0.23	0.12	0.43	1.98	0.18	98.58
	1*s* (*n* = 4)	0.16	0.02	0.05	0.12	0.04	0.01	0.01	0.06	0.01	0.81	0.13		0.01	0.56		
Fragment 6	mean	33.37	0.55	34.39	14.73	1.20	0.18	0.13	2.05	0.04	9.34	0.26	0.12	0.42	1.68	0.18	98.28
	1*s* (*n* = 4)	0.16	0.01	0.10	0.13	0.04	0.02	0.01	0.04	0.01	0.72	0.08		0.03	0.37		
Schorl grand mean		**33.3**	**0.55**	**34.2**	**14.9**	**1.19**	**0.21**	**0.14**	**2.02**	**0.04**	**9.64**	**0.26**	**0.12**	**0.43**	**1.62**	**0.18**	**98.43**
	1*s* (*n* = 24)	0.25	0.03	0.60	0.67	0.10	0.08	0.03	0.08	0.01	0.65	0.08		0.05	0.49		
	1*s* (%)	0.75	5.71	1.77	4.50	8.40	37.25	17.80	3.99	22.49	6.74	29.33		11.50	30.33		
Dyar *et al* . (2001)	*mean*	*33.4*	*0.57*	*33.1*	*17.3*	*1.20*	*0.21*	*0.11*	*1.92*	*0.02*	**11.4*	nd	nd	nd	nd	–	87.88
DRAVITE 108796.1																	
	Potsdam																
Fragment 1	mean	33.05	1.58	20.88	15.63	0.08	7.86	2.41	1.60	0.10	9.60	nd	nd	nd	nd	–	92.79
	1*s* (*n* = 4)	0.31	0.06	0.18	0.39	0.10	0.08	0.11	0.04	0.03	0.32						
Fragment 2	mean	33.39	1.52	22.38	13.76	0.03	8.28	2.30	1.71	0.06	10.44	nd	nd	nd	nd	–	93.86
	1*s* (*n* = 4)	0.28	0.08	0.22	0.62	0.05	0.15	0.09	0.04	0.04	0.45						
Fragment 3	mean	33.20	1.49	22.31	13.91	0.02	8.11	2.39	1.74	0.06	10.21	nd	nd	nd	nd	–	93.43
	1*s* (*n* = 4)	0.29	0.17	0.20	0.13	0.04	0.13	0.08	0.07	0.04	0.26						
Fragment 4	mean	33.30	1.53	21.33	15.31	0.00	8.14	2.59	1.47	0.06	9.93	nd	nd	nd	nd	–	93.65
	1*s* (*n* = 4)	0.07	0.10	0.21	0.79	0.00	0.11	0.06	0.08	0.01	0.39						
Fragment 5	mean	32.81	1.53	20.87	15.47	0.05	8.16	2.67	1.43	0.05	10.57	nd	nd	nd	nd	–	93.60
	1*s* (*n* = 4)	0.33	0.08	0.28	0.63	0.05	0.20	0.08	0.05	0.02	0.34						
Fragment 6	mean	33.24	1.49	22.09	14.78	0.08	8.25	2.29	1.76	0.10	10.13	nd	nd	nd	nd	–	94.20
	1*s* (*n* = 4)	0.19	0.11	0.17	0.41	0.09	0.08	0.09	0.03	0.02	0.28						
Dravite grand mean		**33.16**	**1.52**	**21.64**	**14.81**	**0.05**	**8.13**	**2.44**	**1.62**	**0.07**	**10.15**						**93.59**
	1*s* (*n* = 24)	0.33	0.11	0.69	0.93	0.07	0.20	0.17	0.14	0.03	0.48						
	1*s* (%)	0.99	7.47	3.19	6.30	161.86	2.40	6.92	8.89	50.00	4.74						
DRAVITE 108796.1																	
	Madison																
Fragment 1	mean	34.10	1.60	23.40	13.89	0.01	8.92	2.32	1.69	0.06	10.37	bdl	bdl	0.46	1.93	0.19	98.55
	1*s* (*n* = 4)	0.14	0.02	0.10	0.25	0.01	0.04	0.02	0.03	0.01	0.74			0.02	0.67		
Fragment 2	mean	33.79	1.86	21.87	16.24	-0.02	8.30	2.72	1.50	0.06	10.00	bdl	bdl	0.37	2.43	0.16	98.99
	1*s* (*n* = 4)	0.23	0.02	0.07	0.14	0.01	0.09	0.02	0.03	0.01	0.24			0.02	0.10		
Fragment 3	mean	34.29	1.59	23.36	13.86	0.03	8.93	2.32	1.72	0.06	9.88	bdl	bdl	0.50	2.19	0.21	98.52
	1*s* (*n* = 4)	0.15	0.04	0.19	0.24	0.01	0.12	0.02	0.07	0.01	0.22			0.02	0.17		
Fragment 4	mean	34.50	1.72	23.41	14.28	0.00	8.48	2.46	1.64	0.07	10.18	bdl	bdl	0.47	2.07	0.20	99.07
	1*s* (*n* = 4)	0.21	0.01	0.07	0.15	0.02	0.03	0.02	0.02	0.00	0.39			0.02	0.33		
Fragment 5	mean	33.79	1.61	22.32	15.85	0.00	8.27	2.53	1.59	0.07	9.54	bdl	bdl	0.38	2.52	0.16	98.31
	1*s* (*n* = 4)	0.18	0.03	0.09	0.14	0.02	0.15	0.04	0.06	0.00	0.17			0.02	0.18		
Fragment 6	mean	33.73	1.59	22.50	15.56	0.02	8.31	2.48	1.61	0.05	9.66	bdl	bdl	0.38	2.60	0.16	98.34
	1*s* (*n* = 4)	0.13	0.02	0.02	0.15	0.02	0.09	0.02	0.09	0.01	0.44			0.04	0.34		
Dravite grand mean		**34.0**	**1.66**	**22.8**	**14.9**	**0.01**	**8.53**	**2.47**	**1.63**	**0.06**	**9.94**	**bdl**	**bdl**	**0.43**	**2.29**	**0.18**	**98.63**
	1*s* (*n* = 24)	0.33	0.10	0.63	1.0	0.02	0.30	0.14	0.09	0.01	0.47						
	1*s* (%)	1.0	6.3	2.8	6.7	314	3.5	5.7	5.3	17	4.7						
Dyar *et al* . (2001)	*mean*	*34.7*	*1.6*	*22.0*	*14.1*	–	*8.7*	*2.5*	*1.5*	*0.05*	**10.9*	nd	nd	nd	nd	–	85.23
Frondel *et al. (1966)*		*34.6*	*1.56*	*22.1*	*14.2*	*trace*	*8.69*	*2.36*	*1.41*	*0.1*	*10.42*	nd	nd	nd	nd	–	95.48
ELBAITE 98144.1																	

	Potsdam																
Fragment 1	mean	35.23	0.12	35.57	5.64	0.45	0.89	0.16	2.68	0.02	10.85	nd	nd	nd	nd	–	91.60
	1*s* (*n* = 4)	0.53	0.03	0.21	0.24	0.12	0.05	0.03	0.09	0.01	0.43						
Fragment 4	mean	35.22	0.20	35.27	6.12	0.45	1.12	0.11	2.66	0.03	10.74	nd	nd	nd	nd	–	91.92
	1*s* (*n* = 4)	0.20	0.03	0.46	0.27	0.17	0.07	0.05	0.05	0.01	0.24						
Fragment 5	mean	34.86	0.56	33.85	6.25	0.07	2.86	0.11	2.71	0.02	10.02	nd	nd	nd	nd	–	91.30
	1*s* (*n* = 4)	0.40	0.06	0.20	0.62	0.01	0.08	0.02	0.03	0.01	0.33						
Fragment 6	mean	34.71	0.28	35.34	6.70	0.42	1.11	0.06	2.67	0.03	10.58	nd	nd	nd	nd	–	91.90
	1*s* (*n* = 4)	0.15	0.03	0.37	0.26	0.05	0.13	0.02	0.09	0.01	0.27						
Fragment 10	mean	35.08	0.53	32.84	6.99	0.11	3.56	0.06	2.65	0.04	10.72	nd	nd	nd	nd	–	92.56
	1*s* (*n* = 4)	0.30	0.02	0.14	0.18	0.14	0.03	0.06	0.06	0.03	0.36						
Fragment 12	mean	35.12	0.40	34.34	6.35	0.14	1.86	0.06	2.72	0.03	10.82	nd	nd	nd	nd	–	91.84
	1*s* (*n* = 4)	0.36	0.04	0.19	0.13	0.08	0.03	0.02	0.09	0.03	0.34						
Elbaite grand mean		**34.96**	**0.34**	**34.67**	**6.31**	**0.28**	**1.54**	**0.08**	**2.67**	**0.03**	**10.63**						**91.85**
	1*s* (*n* = 24)	0.40	0.17	1.03	0.55	0.20	1.02	0.06	0.08	0.02	0.45						
	1*s* (%)	1.15	48.60	2.99	8.63	74.95	53.54	59.59	2.93	79.12	4.20						
ELBAITE 98144.1 (non-green)																	
	Madison																
Fragment 1	mean	36.14	0.56	36.07	6.72	0.13	2.98	0.07	2.63	0.02	10.21	bdl	1.97	1.23	0.38	0.52	98.59
	1*s* (*n* = 4)	0.17	0.02	0.08	0.09	0.04	0.08	0.01	0.03	0.01	0.28			0.02	0.35		
Fragment 2	mean	36.01	0.64	34.91	7.22	0.11	3.74	0.06	2.63	0.03	9.27	bdl	1.97	1.14	1.02	0.48	98.25
	1*s* (*n* = 4)	0.09	0.03	0.05	0.11	0.03	0.06	0.01	0.06	0.01	0.27			0.04	0.16		
Fragment 3	mean	36.01	0.28	37.40	6.24	0.39	1.08	0.13	2.67	0.02	10.69	bdl	1.97	1.42	0.55	0.60	98.25
	1*s* (*n* = 4)	0.17	0.03	0.15	0.05	0.04	0.02	0.01	0.02	0.01	0.56			0.04	0.22		
Fragment 4	mean	36.14	0.27	37.44	7.14	0.34	0.76	0.11	2.70	bdl	9.46	bdl	1.97	1.43	1.12	0.60	98.27
	1*s* (*n* = 4)	0.22	0.02	0.15	0.09	0.03	0.02	0.01	0.06	–	0.26			0.02	0.29		
Fragment 5	mean	36.16	0.30	37.53	6.55	0.38	1.03	0.12	2.72	0.02	10.73	bdl	1.97	1.42	0.05	0.60	98.39
	1*s* (*n* = 4)	0.23	0.02	0.13	0.11	0.03	0.03	0.01	0.10	0.00	0.91			0.01	0.85		
Fragment 6	mean	35.97	0.64	34.93	7.33	0.10	3.66	0.06	2.71	0.03	10.29	bdl	1.97	1.13	0.39	0.48	98.73
	1*s* (*n* = 4)	0.18	0.03	0.17	0.10	0.02	0.05	0.01	0.08	0.01	0.72			0.02	0.57		
Elbaite (non-green) grand mean		**36.07**	**0.45**	**36.38**	**6.87**	**0.24**	**2.21**	**0.09**	**2.67**	**0.02**	**10.11**	**bdl**	**1.97**	**1.30**	**0.59**	**0.55**	**98.41**
	1*s* (*n* = 24)	0.18	0.17	1.17	0.41	0.14	1.31	0.03	0.07	0.01	0.76			0.14	0.57		
	1*s* (%)	0.50	38.30	3.23	5.96	56.38	59.25	35.16	2.54	42.44	7.51			10.67	96.63		

ELBAITE 98144.1 (green)																	
	Madison																
Fragment 1	mean	35.41	0.17	38.13	6.15	0.59	0.85	0.13	2.64	0.02	9.86	bdl	1.97	1.40	1.06	0.59	97.80
	1*s* (*n* = 4)	0.04	0.02	0.17	0.14	0.02	0.02	0.01	0.02	0.01	0.45			0.03	0.19		
Fragment 2	mean	36.12	0.17	37.74	6.02	0.54	0.85	0.14	2.69	0.02	10.37	bdl	1.97	1.46	0.65	0.62	98.13
	1*s* (*n* = 4)	0.05	0.01	0.10	0.09	0.03	0.04	0.01	0.04	0.00	0.41			0.04	0.25		
Fragment 3	mean	36.02	0.08	37.81	6.57	0.61	0.34	0.15	2.71	0.01	9.57	bdl	1.97	1.51	0.79	0.64	97.50
	1*s* (*n* = 4)	0.08	0.01	0.15	0.05	0.03	0.02	0.02	0.01	0.01	0.49			0.04	0.15		
Fragment 4	mean	35.94	0.10	37.60	6.61	0.57	0.33	0.16	2.69	0.02	10.03	bdl	1.97	1.48	1.17	0.62	98.05
	1*s* (*n* = 4)	0.23	0.01	0.11	0.13	0.04	0.02	0.01	0.04	0.01	0.59			0.05	0.38		
Elbaite (green) grand mean		**35.87**	**0.13**	**37.82**	**6.34**	**0.58**	**0.59**	**0.14**	**2.69**	**0.02**	**9.96**	**bdl**	**1.97**	**1.46**	**0.92**	**0.62**	**97.87**
	1*s* (*n* = 16)	0.30	0.05	0.23	0.28	0.04	0.27	0.02	0.04	0.01	0.53			0.06	0.32		
	1*s* (%)	0.85	35.36	0.62	4.46	6.40	44.89	10.56	1.50	44.24	5.35			3.84	34.36		
Dyar *et al.* (2001)	*mean*	*36.5*	*0.43*	*35.0*	*6.36*	*0.21*	*2.12*	*0.09*	*2.55*	*0.02*	**8.3*						83.24
NIST SRM 610 glass																	
	Potsdam																
	mean	66.49	0.08	1.78	0.10	0.10	0.08	11.20	12.74	0.06	1.07	nd	nd	nd	nd	–	93.70
	1*s* (*n* = 13)	0.51	0.06	0.05	0.10	0.07	0.03	0.24	0.23	0.04	0.39						
	1*s* (%)	0.77	81.64	2.54	96.73	78.15	39.58	2.16	1.79	63.10	36.05						
Jochum *et al.* (2011)	preferred	69.70		1.95				11.40	13.40								

Values are in % *m/m* , total Fe calculated as FeO, all data reported in online supporting information Table S1.

*B_2O_3 values from Dyar *et al.* (2001) are from the GFZ laboratory and should be superseded by those reported here.

bdl = below detection limits

nd = not determined

Instruments and analytical conditions used: GFZ Potsdam, July 2019, JEOL Hyperprobe JXA-8500F with field-emission cathode and five wavelength-dispersive spectrometers, 10 kV accelerating voltage, 10 nA beam current, 8–10 µm beam diameter. Counting times for peaks/background were 60/30 s for B, 20/10 s for Fe, Mn, Ti and 10/5 s for Na, Ca, Mg, Si, Al and K. Calibration materials: schorl (B, Si, Al, Fe), orthoclase (K), diopside (Ca, Mg), rhodonite (Mn), rutile (Ti), and tugtupite (Na). Only Ka-Lines were used, with the first sequence: B (LDEB), Fe (LIF), K (PETJ), Al (TAP), Si (PETH); and second: Mn (LIF), Ca (PETJ), Na (TAP); lastly Ti (LIF) and Mg (TAP). Relative analytical uncertainties (1*s*) are ~ 1% for Si, ~ 3% for Al and < 5% for B. Deviation of NIST SRM 610 SiO_2 from the recommended value (Jochum *et al* . 2011) is due to Si being calibrated on tourmaline. Data reduction used the ϕ(ρZ) correction scheme (CITZAF; Armstrong 1995).

Analyses at UW-Madison in February 2020 by CAMECA SXFive FE with five wavelength-dispersive spectrometers and Probe for EPMA software. Two conditions were utilised: 7 kV accelerating voltage, 40 nA and 10 µm defocused beam for O, B, and F; 15 kV, 20 nA and 10 µm defocused beam for the balance of the elements. Counting times were 10 seconds on peak and 5 s each on two background positions. Boron was measured with PC2 (98Å 2d) and O and F with PC0 (45 Å 2d) layered synthetic diffractors. A small overlap of Fe L upon F Ka was corrected inside the matrix correction, which was the full PAP phi-rho-Z. The mass absorption coefficients of Bastin and of Pouchou for B, O and F by the other elements were applied. Calibration materials were: NIST SRM K326 (B), Burma jadeite--London Natural History Museum (Na, Al, Si, O), NIST K411 glass (Mg, Ca), Harvard University haematite (Fe), Asbestos microcline (K), syntheitic TiO2 (Ti), syntheitic tephroite (Mn), synthetic ZnO (Zn) and Thomas Range F-topaz (F). The tourmalines fragments and the standards were mounted together in the same mount and carbon coated with ~ 200 nm of carbon (polished brass colour technique). Minimum detection limits (MDLs) for the following low concentration oxides for each individual spot analysis were: K_2O 0.02, CaO 0.02, TiO_2 0.03, and ZnO 0.13% *m/m* . Differential PHA with wide windows was used for O, B and F, whereas integral PHA was used for the other elements. For the purposes of matrix correction, Li_2O was also input into the composition of the tourmaline fragments, based upon the values presented elsewhere in this paper. After all of the measured oxygen was accounted for by stoichiometric appropriation (including Fe as FeO), any remaining oxygen was assigned to OH. These OH values are considered appropriate for purposes of the matrix correction.

Table 2.

Summary of SIMS homogeneity tests for lithium mass fraction and new working value

				Li_2O (% *m/m*)				
		$^{7}Li^{+}/^{28}Si^{+}$	Precision [b]	This study [c]	Dyar 1	Dyar 2	Dyar 3	Dyar 4
SCHORL 112566.1	mean	0.1403	0.81%	0.1176	0.09	0.107	0.071	nr
	1*s* (*n* = 30)	0.0105		0.0087				
	% RSD [a]	7.4		7.4				
DRAVITE 108796.1	mean	0.00207	1.94%	0.00177	nr	0.017	0.00095	0.0013
	1*s* (*n* = 28)	0.00028		0.00024				
	% RSD [a]	13.6		13.6				
ELBAITE 98144.1	mean	2.12	0.27%	1.92	1.33	0.98	0.30	nr
	1*s* (*n* = 36)	0.21		0.19				
	% RSD [a]	9.8		9.8				
NIST SRM 610	mean	0.0567	0.68%					
	1*s* (*n* = 19)	0.0015						
	% RSD [a]	2.6						

nr = not reported

a. Repeatability from "*n* " repeat measurements. See online Table S2 for information about the distribution of SIMS results.
b. Mean "internal precision" from twenty cycles per measurement (1SE).
c. Lithium mass fractions calibrated from NIST SRM 610 glass, recommended SiO_2 value 69.4% *m/m* and Li 468 μg g^{-1} (Jochum *et al.* 2011). SiO_2 values for tourmalines used in calculation is the mean of Potsdam and Madison values (see Table 1).
d. Lithium mass fractions reported by Dyar *et al* . (2001) based on (1) PIGE, (2) flame AAS, (3) SIMS, (4) ICP-AES.

Table 3.

Summary of SIMS homogeneity tests for lithium isotope ratio

		$^{7}Li / ^{6}Li$	Cycles	Precision [b]	Beam current	^{7}Li cps	Detector [c]	Test mass (ng) [d]
SCHORL 112566.1	mean	11.6316	50	0.17 ‰	3.5 nA	3.9E+06	EM/FC	0.10
	1*s* (*n* = 44)	0.0087						
	RSD [a]	0.75‰						
DRAVITE 108796.1	mean	12.16830	150	0.3 ‰	12 nA	1.9E+05	EM/EM	1.3
	1*s* (*n* = 36)	0.02630						
	RSD [a]	2.16‰						
ELBAITE 98144.1	mean	12.71700	25	0.08 ‰	4.5 nA	7.6E+07	FC/FC	~ 0.07
	1*s* (*n* = 38)	0.00430						
	RSD [a]	0.33‰						
NIST SRM 610	mean	11.81660	50	0.08 ‰	3.5 nA	2.6E+06	EM/FC	nd
	1*s* (*n* = 8)	0.00500						
	RSD [a]	0.43‰						

n = number of determinations, this also includes the data from the small "DM" area

nd = not determined

Values for beam current, ^{7}Li count rate and internal precision are the mean of "*n* " measurements.

All data are reported in online supporting information Table S3.

a. Repeatability from "*n* " repeat measurements as 1*s* (in ‰).

b. "Internal" precision from "*n* " cycles as 1SE / mean in permil.

c. Ion detection method: EM = electron multiplier, FC = Faraday cup.

d. Amount of material sputtered based on white light profilometry and an assumed density of $\rho = 3.0$ g cm^{-3}

Table 4.

Summary of SIMS homogeneity tests for oxygen isotope ratio

		$^{18}O / ^{16}O$ (meas.)	$^{18}O / ^{16}O$ (corr.) [b]	Precision [c]	IMF [d]	IMF uncert. [E]
SCHORL 112566.1	mean	0.00201780	0.00201709	0.11‰	0.99630	0.030
	1*s* (*n* = 63)	5.47E-07	5.39E-07			
	RSD [a]	0.27‰	0.27‰			
DRAVITE 108796.1	mean	0.00202194	0.00202103	0.10‰	0.99785	0.1
	1*s* (*n* = 47)	5.12E-07	4.42E-07			
	RSD [a]	0.25‰	0.22‰			
ELBAITE 98144.1	mean	0.00202725	0.00202645	0.11‰	0.99825	0.0
	1*s* (*n* = 70)	6.12E-07	4.55E-07			
	RSD [a]	0.30‰	0.22‰			
NIST SRM 610	mean	0.00203007	0.00202942	0.10‰	1.0	
	1*s* (*n* = 29)	6.68E-07	4.28E-07			
	RSD [a]	0.33‰	0.21‰			

All data are reported in online supporting information Table S4.

a. Repeatability from "*n* " measurements (1*s*).

b. Corrected for linear drift based on NIST SRM 610 measurement results (see text for details).

c. Mean "internal precision" from "*n* " cycles (1SE).

d. $^{18}O/^{16}O$ instrumental mass fractionation (measured ratio / true), based on the grand mean $\delta^{18}O$ values indicated in Table 6.

e. Uncertainty in ‰ of the recomended δ value of this material (see Table 7).

Table 5.

Summary results of $\delta^7Li_{L\text{-}SVEC}$ by solution ICP mass spectrometry, values in ‰

Material	Laboratory	Dissolution	No. of analyses	δ^7Li (mean) ‰	δ^7Li (range) ‰	1*s*	Lin *et al* . (2019)[b]
SCHORL 112566.1	Bremen	1	5	5.71	5.52–5.88	0.13	
	Maryland	1	2	4.24	4.22–4.26	nd	
	Maryland	2	2	4.81	4.64–4.98	nd	
	Bristol	1	2	5.64	5.60–5.72	nd	
	Bristol	2	2	5.71	5.64–5.78	nd	
	Woods Hole	1	4	5.52	5.35–5.70	0.15	
	Woods Hole	2	4	5.29	4.70–5.66	0.37	
	Median[a]			5.52 ± 0.23			6.47 ± 0.20
DRAVITE 108796.1	Bremen	1	2	10.99	nd	nd	
	Maryland	1	2	8.72	7.97–9.35	nd	
	Maryland	2	1	8.78	8.21–9.34	nd	
	Bristol	1	3	10.17	10.10–10.25	0.07	
	Bristol	2	2	10.24	10.14–10.35	nd	
	Woods Hole	1	1	9.67	nd	nd	
	Woods Hole	2	1	10.24	nd	nd	
	Median[a]			10.17 ± 0.34			
ELBAITE 98144.1	Bremen	1	5	7.10	6.94–7.28	0.13	
	Maryland	1	2	6.04	5.84–6.24	nd	
	Maryland	2	2	6.87	6.64–7.11	nd	
	Bristol	1	3	7.18	7.12–7.24	nd	
	Bristol	2	2	7.71	7.62–7.81	nd	
	Woods Hole	1	4	7.13	6.80–7.34	0.23	
	Median[a]			7.12 ± 0.24			7.90 ± 0.22

See online supporting information Table S5 for a complete report of all individual results.

nd = not defined, 1*s* repeatability values only reported for those aliquots with ≥ 3 mass spectrometer determinations.

a. Median of n = 6 or 7 independent dissolutions with 1SE based on the 1*s* reproducibility divided by √(n - 1).

b Values in ‰ reported by Lin *et al*. (2019) for comparison based on n = 3 determinations using microdrilling and wet chemical methods; uncertainty estimates are 1*s*.

Table 6.

Summary results of oxygen isotope ratio analyses by gas source mass spectrometry

				$\delta^{18}O_{SMOW}$		$\delta^{17}O_{SMOW}$	
Material	Laboratory	Session	*n* [b]	Mean	Range [c]	Mean	Range [c]
SCHORL 112566.1	Cape Town	1	2	9.59	9.54–9.64		
	Cape Town	2	2	9.75	9.66–9.83		
	Milton Keynes	1	2	9.71	9.68–9.74	5.07	5.05–5.08
	Milton Keynes	2	2	9.71	9.71–9.71	5.07	5.06–5.08
	Madison	1	2	9.76	9.74–9.77		
	Madison	2	2	9.63	9.58–9.67		
	Keyworth	1	2	9.49	9.74–9.61		
	Keyworth	2	2	9.65	9.33–9.97		
	Keyworth	3	1	9.46			
	E. Kilbride	1	3	9.70	9.59–9.78		
	Göttingen	1	1	9.81		5.12	
	Göttingen	2	2	9.70	9.47–9.81	5.06	4.93–5.12
	Grand Mean[a]			9.66 ± 0.03		5.08	
Dyar *et al* . (2001)				10.32 ± 0.03			
DRAVITE 108796.1	Cape Town	1	2	9.99	9.98–9.99		
	Cape Town	2	2	10.01	9.90–10.12		
	Milton Keynes	1	1	10.04		5.38	
	Milton Keynes	2	2	10.07	10.02–10.12	5.27	5.24–5.29
	Madison	1	2	10.19	10.17–10.20		
	Madison	2	2	10.01	9.99–10.02		
	Keyworth	1	2	9.75	9.50–10.0		
	Keyworth	2	2	10.62	10.59–10.74		
	E. Kilbride	1	4	9.92	9.80–9.99		
	Göttingen	1	3	10.13	10.12–10.16	5.29	5.28–5.31
	Grand Mean[a]			10.07 ± 0.08		5.31	
Dyar *et al* . (2001)				10.03 ± 0.02			

ELBAITE 98144.1	Cape Town	1	2	13.71	13.69–13.73		
	Cape Town	2	2	13.74	13.71–13.77		
	Milton Keynes	1	2	13.81	13.77–13.85	7.21	7.18–7.23
	Milton Keynes	2	2	13.87	13.87–13.87	7.24	7.23–7.25
	Madison	1	3	13.87	13.81–13.92		
	Madison	2	2	13.96	13.84–14.08		
	Keyworth	1	1	14.52			
	Keyworth	2	1	12.72			
	Keyworth	3	1	13.73			
	E. Kilbride	1	4	13.54	13.20–13.79		
	Göttingen	1	3	13.94	13.82–14.00	7.27	7.20–7.31
	Grand Mean[a]			13.76 ± 0.13		7.24	
Dyar *et al* . (2001)				13.89 ± 0.02			
UWG-2 grnt	Cape Town		4	5.76	5.69–5.87		
	Milton Keynes		4	5.75	5.69–5.80	2.98	2.96–3.01
	Madison		4	5.80	5.75–5.91		
	Keyworth		3	5.49	5.07–5.98		
	E. Kilbride		9	5.75	5.63–5.87		
	Göttingen		15	5.77	5.62–5.90	2.99	2.93–3.06
See online supporting information Table S6 for a complete report of all individual results.							
a. simple mean of *n* = 10, 11 or 12 independent sessions with 1SE based on the reproducibility divided by √(n - 1).							
b. number of independent determinations during the given measurement session (day).							
c. range only reported for those determinations containing ≥ 2 determinations.							

Table 7.

Compilation of reference values for the three Harvard tourmaline materials

	LiO_2 mass fraction	$\delta^7Li_{L\text{-}SVEC}$	$\delta^{18}O_{SMOW}$	$\delta^{17}O_{SMOW}$	δD [b]	$\delta^{11}B$ [c]	$\delta^{11}B$ [d]
	(% *m/m*) [a]	(‰)	(‰)	(‰)	(‰)	(‰)	(‰)
Schorl 112566.1	0.118 ± 0.009	5.52 ± 0.23	9.66 ± 0.03	5.08	-92.4	-12.5	-13.86
Dravite 108796.1	0.00177 ± 0.00024	10.17 ± 0.34	10.07 ± 0.08	5.31	-47.3	-6.6	-6.86
Elbaite 98144.1	1.92 ± 0.19	7.12 ± 0.24	13.89 ± 0.02	7.28	-99.4	-10.4	-12.02
Status	Current Best Estimate	Recommended Value	Recommended Value	Working Value	Working Value	Published	Published
uncertainty type	1*s* repeatability	1SE	1SE				
a. Values based on SIMS data calibrated using silicate glass NIST SRM 610 -- subject to uncontrolled matrix effects.							
b. Values published by Dyar *et al*. (2001) on starting materials.							
c. Values published by Leeman and Tonarini (2001) on starting material.							
d. Values published by Marger *et al*. (2020) on starting material.							

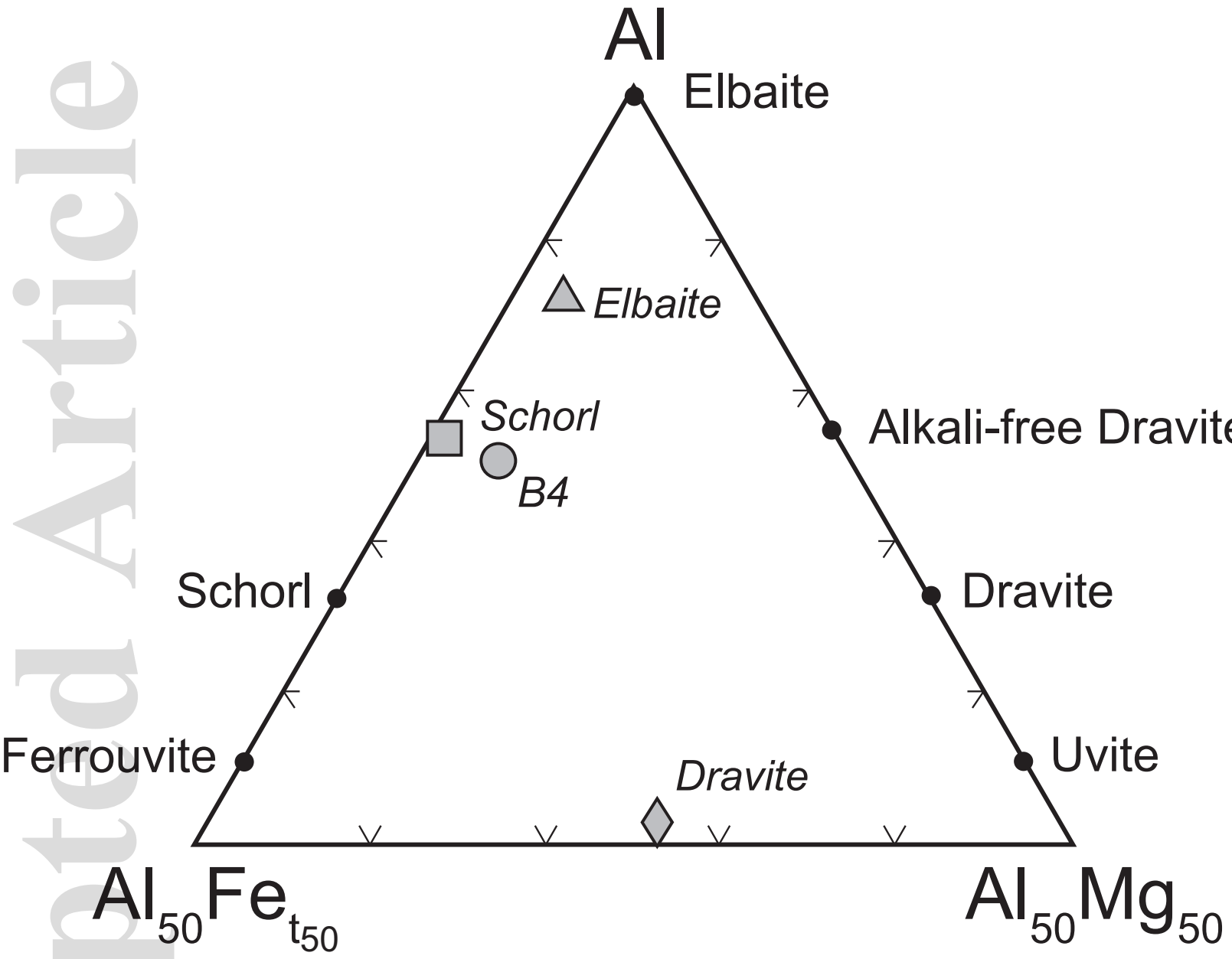

ggr_12362_f1.eps